

Smart Drug Conjugated Silica Nanoparticles for Controlled and Sustained Release

Wanxia Zhao

School of Chemical Engineering



A thesis submitted for the degree of

Master of Philosophy

The University of Adelaide

October 2015

Declaration

I certify that this work contains no material which has been accepted for the award of any other degree or diploma in my name, in any university or other tertiary institution and, to the best of my knowledge and belief, contains no material previously published or written by another person, except where due reference has been made in the text. In addition, I certify that no part of this work will, in the future, be used in a submission in my name, for any other degree or diploma in any university or other tertiary institution without the prior approval of the University of Adelaide and where applicable, any partner institution responsible for the joint-award of this degree.

I give consent to this copy of my thesis, when deposited in the University Library, being made available for loan and photocopying, subject to the provisions of the Copyright Act 1968.

The author acknowledges that copyright of published works contained within this thesis resides with the copyright holder(s) of those works.

I also give permission for the digital version of my thesis to be made available on the web, via the University's digital research repository, the Library Search and also through web search engines, unless permission has been granted by the University to restrict access for a period of time.

Signature: _____ Date: _____

Acknowledgment

I would like to take this opportunity to thank all the people who helped and supported me during my two years Master of Philosophy study at the University of Adelaide. It is their impressive kindness and advices made this thesis possible.

First and foremost, I would like to express my deepest gratitude to my supervisors Associate Professors Sheng Dai and Jingxiu Bi for their valuable guidance, patience and encouragement in every stage of my study. Their effective suggestions, shrewd comments and vigorous academic observation have enlightened me not only in this thesis, but also in my future study and career.

I shall extend my thanks to Dr. Hu Zhang in our research group, who has given me generous helps and suggestions through my study. I would also like to thanks Dr. Xin Du, Mr. Xiaolin Cui, Mr. Bingyang Zhang as well as other research group members from School of Chemical Engineering, the University of Adelaide for their help and support on my experiments. They offer me not only useful discussions and suggestions, but also valuable friendships.

Last but not least, my greatest gratitude must go to my parents who provide me constant encouragement and endless love throughout my life.

Abstract

Drug delivery system (DDS) is crucial for modern cancer treatment. Traditional drug delivery process is to load drugs into various carriers via physical interactions, which always gives rise to the burst release and leakage of the loaded drugs. This thesis aims to develop a novel delivery platform with controlled and sustained drug release ability, where doxorubicin (DOX, a model anticancer drug) is conjugated to the surfaces of model carriers, silica nanoparticles (SNs), via different “smart” linkers. pH and glutathione (GSH) are utilized as the stimuli of these “smart” linkers to construct pH and intracellular microenvironment redox responsive drug-carrier conjugated delivery systems to selectively deliver drugs.

The pH regulated drug delivery system was developed to conjugate DOX to the surfaces of silica nanoparticles by acid responsive hydrazone bonds. The drug delivery system showed good stability under physiological pH of 7.4 to avoid premature drug leakage in blood circulation, and sustained release under acidic extracellular environment of cancer cells to effectively inhibit tumor growth. *In vitro* cytotoxicity study against Hela cells and HEK 293 cells indicated the drug delivery system revealed such a system could release more drugs in tumor cells than normal cells.

The intracellular microenvironment redox responsive drug delivery system was established by introducing dithiodibutyric acid (DTDB), which contained redox responsive disulfide bonds, to silica nanoparticle surfaces. In the absence of reducing

reagents of GSH or dithiothreitol (DTT), such a drug delivery system presented good stability to prevent drug leakage, but in the presence of GSH or DTT, the disulfide bonds could be effectively cleaved to release the preloaded drugs. The *in vitro* cytotoxicity study indicated this drug delivery system could be stable in blood circulation and effectively released the preloaded drugs inside cells after conjugation. Due to the different GSH levels in cancer cells and normal cells, intracellular microenvironment redox responsive system could be more toxic to cancer cells.

In summary, DOX-silica nanoparticles conjugates with pH regulated hydrazone bonds or intracellular microenvironment redox responsive disulfide bonds had the capability in controlled and sustained drug release, which could effectively eliminate drug leakage during the delivery course and release sufficient amount of drugs in tumors to inhibit their growth.

Table of Contents

DECLARATION	I
ACKNOWLEDGMENT	II
ABSTRACT	III
Chapter 1 Introduction	1
1.1 Background	1
1.2 Aims and objectives	4
1.3 Outline of the thesis	5
References	6
Chapter 2 Literature Review	8
2.1 The importance of drug delivery systems in cancer therapy.....	8
2.2 Traditional drug delivery systems using silica nanoparticles.....	10
2.3 Covalent conjugation of drugs to carriers by pH sensitive linkers	15
2.3.1 Amide bonds	16
2.3.2 Hydrazone bond	19
2.4 Drug conjugation by intracellular microenvironment responsive linker	23
2.4.1 Enzyme responsive drug delivery systems	24
2.4.2 Redox responsive drug delivery systems	28
2.5 Summary	31
References	32
Chapter 3 Doxorubicin conjugated silica nanoparticles: A pH regulated delivery system for controlled and sustained drug release	38
Abstract	42
3.1 Introduction	43
3.2 Materials and Methods	45
3.2.1 Materials.....	45

3.2.2 Synthesis of silica nanoparticles	46
3.2.3 Introduction of pH sensitive linker on the surface of silica nanoparticles.	47
3.2.4 Characterization	48
3.2.5 Drug loading and ex vivo doxorubicin release	49
3.2.6 Cytotoxicity.....	50
3.2.7 Fluorescence Imaging Analysis	50
3.3 Results and Discussion.....	51
3.3.1 Synthesis of hydrazine-silica nanoparticles and characterization of surface functional groups	51
3.3.2 Loading DOX to hydrazine-silica nanoparticles by covalent bonds.....	54
3.3.3 pH responsive ex vivo DOX release	54
3.3.4 Cytotoxic evaluation against Hela cells and HEK 293 cells.....	56
3.3.5 Cell uptake analysis by live/dead cell assays.....	57
3.4 Conclusions	59
References	69
Supporting information	73

Chapter 4 Intracellular microenvironment redox-responsive drug-conjugated silica nanoparticles for sustainable drug delivery 76

Abstract	80
4.1 Introduction	81
4.2 Materials and Methods	83
4.2.1 Materials.....	83
4.2.2 Synthesis of monodisperse silica nanoparticles	84
4.2.3 Synthesis of redox sensitive linker modified silica nanoparticles	84
4.2.4 Drug conjugation and ex vivo drug release evaluation.....	85
4.2.5 Cytotoxicity.....	86
4.2.6 Fluorescent Dead/Live cell assays	87
4.2.7 Equipment	88

4.3 Results and Discussion.....	88
4.3.1 Preparation and characterization of SNs-S-S-DOX conjugates	88
4.3.2 Ex vivo redox-responsive triggered cleavage of the SNs-S-S-DOX conjugates by DTT and GSH.....	91
4.3.3 In vitro evaluation of cytotoxicity and cell uptake against HeLa cells and HEK 293 cells	93
4.4 Conclusions	95
References	105
Supporting information	108
Chapter 5 Conclusions and Recommendation	110
5.1 Conclusions	110
5.2 Future recommendation	112

Chapter 1 Introduction

1.1 Background

Over the past decades, with the research development in pharmaceutical drugs, more knowledge of the drug properties for various diseases has been obtained as well as the mechanisms of cellular uptake, which make the contribution in therapeutic efficiency improvement. Nevertheless, in some cases including chemotherapy for cancer, conventional cytotoxic drugs are still widely used as the primary treatment method, which provides limited effectiveness with numerous adverse side effects. The chemotherapy cancer treatment needs the use of high dosages of cytotoxic drugs, and because of the lack of specificity, the drugs bring toxic effect to healthy cells that results in significant side effects.¹ In order to overcome this problem, one of the most popularly used methods is the development of drug delivery systems (DDS) with targeting ability. The ideal drug delivery systems are able to deliver sufficient amount of drugs to target sites and achieve its desired therapeutic effect with minimized side effects. Besides the quantity of drugs, drug delivery system also concerns about the duration of drugs presence and the route of drug taken into body.²

Since the increasing significance of the application of DDS, nowadays, many researches have focused on constructing effective drug delivery systems using biocompatible carriers with high drug load capability, less premature release and specific target controlled release. To achieve this goal, various functional organic materials, such as

polymers, liposomes, and dendrimers, have been investigated to construct smart drug delivery systems.^{1,3} However, for these soft organic delivery materials, the distortion and degradation of carriers during blood circulation always give rise to the leakage of preloaded drug during delivery. Therefore, inorganic materials, which have stable structures to protect the loaded drugs, are taken into consideration. Among them, silica nanoparticles (SNs) with uniform structures and multifunctional surface properties have been widely recognized as one of the feasible drug carriers because its surface can be easily modified with different functional groups to load drugs or conjugate targeting molecules.^{4,5}

For the traditional approach of using silica nanoparticles as delivery carriers, most successful strategies are based on mesoporous silica nanoparticles (MSNs). After drug loading to the mesopores of MSNs, diverse nanocaps are utilized to cap the pores to eliminate drug leakage. The caps can be opened or closed by the treatment of either internal stimuli, including pH, temperature and enzyme, or external stimuli, including light, heat and magnetic field, to control the drug release.⁶ Despite of its proven effectiveness and advantage of potential to achieve low premature release, this stimuli responsive strategy always suffers from the poor controlled release profiles, such as the burst drug release associated with the formation of weak drug-carrier physical bonds.⁷

In order to overcome this problem, conjugation of drugs to carriers through various stimuli sensitive linkers may provide additional advantages over traditional drug delivery

systems. Due to the presence of strong and stable covalent bonds, the loaded drugs are difficult to leak during drug administration and will experience a slow sustainable release profile.⁸

Although many stimuli responsive systems using temperature, light, chemical agents and magnetic fields to trigger drug release, pH and intercellular micro-environment responsive system are most of particular interest and receiving growing attention for drug-carrier conjugation systems. The extracellular pH of cancer cells is around 5.0, which is more acidic than the physiological pH of 7.4 in blood and normal tissues.^{9, 10} For the intracellular microenvironment redox responsive systems, the concentration of reduction glutathione (GSH) in the cancer cells is 10 times higher than the normal cells and 1000 times higher than the plasma.¹¹ For the intracellular microenvironment enzyme-responsive systems, the existence of special enzyme in abnormal cells can be used to trigger the cleavage of smart linkers. The different concentrations of these triggers make them be feasible as the smart stimuli to effectively control the target drug release and prevent premature leakage. Nowadays, most studies have been reported to establish pH, redox and enzyme responsive systems based on polymer materials. However, soft polymeric delivery systems result in distortion and degradation associated with blood circulation, and redox responsive systems seem to be more feasible to achieve sustainable drug release than enzyme responsive systems.

Herein, this thesis will be addressing the synthesis and evaluation of drug-silica

nanoparticles conjugates in the presence of pH and redox responsive linkers. Doxorubicin (DOX) is chosen as a model drug, and it will be conjugated to the surface of silica nanoparticles through various surface modification and functionalization. Materials characterization, drug loading, drug release behaviors and cytotoxicity of these smart delivery systems will be evaluated. The detailed comparison on pH and intercellular micro-environment redox responsive systems will be discussed to guide future development of high performance drug delivery systems for cancer treatment.

1.2 Aims and objectives

This work aims to prepare the silica nanoparticle based drug delivery system for cancer treatment. Considering the defects of traditional drug delivery approach, this work focuses on synthesizing the novel DOX-silica nanoparticles conjugated drug delivery systems with either pH or intracellular redox responsive linkers, and use them as feasible drug delivery carriers to avoid premature drug linkage during delivery.

In order to achieve this aim, the following objectives have been launched in the thesis:

- Identify the most suitable pH responsive or microenvironment redox-responsive linkers to conjugate drugs on silica nanoparticle surfaces;
- Surface modification on silica nanoparticles with the selected pH or redox sensitive linkers, and followed by drug conjugation;

- Physical and chemical characterization of synthetic materials, evaluating the cytotoxicity, drug loading, and controlled release behaviors of the above systems;
- Discuss the potential and feasibility of the above systems to achieve sustainable release.

1.3 Outline of the thesis

This thesis is prepared by paper-basis and detailed structures are outline below:

Chapter 1 introduces with background information, research gaps, aims, objectives and thesis outline. Chapter 2 is a literature review. Current development of traditional drug delivery systems and the recent achievement in pH and intracellular micro-environment responsive drug delivery systems have been systematically analyzed and discussed. Chapter 3 and 4 are Results and Discussion section, where Chapter 3 reports the synthesis and evaluation of a pH regulated drug delivery system based on the DOX-silica nanoparticles conjugates with pH responsive hydrazone bond. Chapter 4 describes the preparation and evaluation of an intracellular redox micro-environment responsive drug conjugated silica nanoparticles with glutathione (GSH) sensitive disulfide bonds. Finally, Chapter 5 concludes the thesis and future recommendations are proposed.

References

1. M. Colilla, B. González and M. Vallet-Regí *Biomaterials Science*, 2013, **1**, 114-134.
2. I. Slowing, J. L. Vivero-Escoto, C. W. Wu and V. S. Lin, *Advanced Drug Delivery reviews*, 2008, **60**, 1278-1288.
3. C. H. Tsai, J. L. Vivero-Escoto, Slowing, II, I. J. Fang, B. G. Trewyn and V. S. Lin, *Biomaterials*, 2011, **32**, 6234-6244.
4. V. Mamaeva, C. Sahlgren and M. Linden, *Advanced Drug Delivery Reviews*, 2013, **65**, 689-702.
5. J. Gu, S. Su, M. Zhu, Y. Li, W. Zhao, Y. Duan and J. Shi, *Microporous and Mesoporous Materials*, 2012, **161**, 160-167.
6. J. E. Lee, D. J. Lee, N. Lee, B. H. Kim, S. H. Choi and T. Hyeon, *Journal of Materials Chemistry*, 2011, **21**, 16869-16872.
7. C. Loira-Pastoriza, J. Todoroff and R. Vanbever, *Advanced Drug Delivery Reviews*, 2014, **75**, 81-91.
8. D. W. Dong, S. W. Tong and X. R. Qi, *Journal of Biomedical Materials Research. Part A*, 2013, **101**, 1336-1344.
9. C. Lu, B. Li, N. Liu, G. Wu, H. Gao and J. Ma, *RSC Advances.*, 2014, **4**, 50301-50311.

10. A. Thistlethwaite, D. Leeper, D. Moylan and R. Nerlinger, *Radiation Oncology*

Biology Physics, 1985, **11**, 1647-1652.

11. Z. B. Zheng, G. Zhu, H. Tak, E. Joseph, J. L. Eiseman and D. J. Creighton,

Bioconjugate Chemistry, 2005, **16**, 598-607.

Chapter 2 Literature Review

2.1 The importance of drug delivery systems in cancer therapy

Cancer is the first or second leading cause of death in Australia. According to the Cancer Council Australia, in 2012, cancer had caused the death of more than 43,000 Australians, which accounted for almost one third the total deaths in Australia. In 2015, around 128,000 new cases of cancer are predicted to be diagnosed, while this number may continually increase to 150,000 in 2020. Therefore, extensive efforts have been made in cancer treatment, which costs enormous amount of money. From 2000 to 2001, more than 22 % of health research expenditure of \$378 million has been spent on the research of cancer. In 2014, the statistical cancer treatment cost was more than \$4.5 billion, which took 6.9 % of the total health system costs.¹

Currently, the methods that are widely used in cancer therapy include surgery removal, radiation and chemotherapy.^{2, 3} Surgery operation can only remove the tumors with large enough size but cannot remove the cancer cells in the deposits of tumors, which always results in recurrence. The radiation therapy can be used to treat on certain areas of body, but its damage to normal tissues including skin changes and fatigue are irreversible.² Chemotherapy plays a significant role in the treatment of different staged cancers. Chemotherapy can effectively kill the cancer cells around the body, even the cells that have been transferred to other tissues through the blood circulation, and thus prevent the recurrence after tumor removal surgically.

However, the effectiveness of conventional chemotherapy is usually limited, which directly results in the consumption of high-dose anticancer drugs.⁴ For example, small sized anticancer drugs can be easily removed from body by quick metabolism and excretion. The low solubility of some anticancer drugs makes it impossible to deliver them directly to cancer cells. Besides, due to the non-specificity of anticancer drugs, normal cells and tissues are also damaged associated with drug administration, which makes patients suffered from serious side effects.³

In order to solve this problem, during the past decades, great efforts have been made to improve the chemotherapeutic efficiency of anticancer drugs. One of the most attractive methods is to construct the smart drug delivery systems (DDS), which are able to effectively and selectively deliver sufficient amount of anticancer drug molecules to tumors.⁵⁻⁷ Using suitable delivery cargos, the drugs can be stabilized and protected by the carriers to increase drug solubility and prevent drug leakage in blood circulation. As a result, the side effects of drugs to normal cells can be minimized. At the same time, the drug delivery systems can also provide the protection to some protein or gene based drugs to avoid their enzymatic degradation and damage during delivery.⁸ Therefore, with the advent of effective drug delivery systems, the desired therapeutic effect can be achieved safely by altering drug release behaviors and distributions.

2.2 Traditional drug delivery systems using silica nanoparticles

Drug delivery systems are designed to transport sufficient amount of drug molecules to the targeted cells as well as prevent undesired drug leakage and degradation during delivery. The success of this method depends on choosing suitable drug carrier materials with the ability of:

1. High drug loading efficiency.
2. Biocompatible or non-cytotoxic to human tissues.
3. Small or zero drug leakage during the delivery course.
4. Target and controlled drug release to cancer cells.⁹

In literature, various biodegradable organic materials, such as amphiphilic polymers, microgels, polymeric nanoparticles, liposomes, dendrimers, and others have been taken into consideration as effective drug carriers.⁹⁻¹¹ Anticancer drugs can be loaded to these carriers through hydrophobic or electrostatic interactions. After administration, these carriers can be degraded as being triggered by various stimuli, such as pH, temperature, redox reagent, external field and others, to release the preloaded drug molecules. Many of these drug delivery systems present satisfied results, but the distortion and degradation of the carriers during blood circulation make the entrapped drugs easy to leak in the delivery. Thus, the zero premature drug release is hard to achieve for these soft organic delivery materials.^{9, 12}

In order to overcome this hurdle, research on the development of inorganic carrier

materials have been reported, which can provide sufficient protection to drug molecules.⁹ Among those inorganic materials, silica nanoparticles (SNs) are receiving high attention and interest to be investigated as effective drug delivery carrier due to its uniform structures, multifunctional properties and biocompatibility.^{5, 13, 14} FDA has approved the application of small silica nanoparticles for biological application, and silica nanoparticles have been reported to be potential to load and controlled release of antibiotics and anticancer drugs.¹⁵⁻¹⁷

Most of the successful cases using silica nanoparticles as delivery carriers are based on the synthesized mesoporous silica nanoparticles (MSNs). Mesoporous silica nanoparticles have been widely applied on drug delivery, which is associated with their suitable pore sizes, large surface areas, good stability, excellent biocompatibility, and easy to prepare and surface modification. The MSNs are generally synthesized by surfactant-templated hydrolysis, where the tetraethoxysilane (TEOS) is used as the silica source and structure directing agent (surfactant) including cetyltrimethylammonium bromide (CTAB) can generate porosity.¹⁸ The resulting MSNs have plenty of hydroxyl (OH) groups on surface, which make it well dispersed in aqueous systems. Moreover, varieties of functional groups can be easily modified at MSNs' surfaces to make the particles more suitable for drug delivery applications. The surface modifications can be conducted by either one-pot co-condensation synthesis, post-synthetic grafting of functional silanes and imprint coating methods.⁹

Due to the presence of mesoporosity, drugs can be easily loaded to MSNs or surface modified MSNs by different approaches. In order to avoid premature leakage and fulfil the release of drugs at the desired position, a ground-breaking strategy of MSN-based stimuli-responsive system using the concept of gatekeeping has been developed.^{14, 19} As shown in Figure 1, the drugs can be first encapsulated into the pores of mesoporous silica nanoparticles. Different nanocaps are then used to cap the ends of pores to prevent premature release. After administration, the gatekeepers can be uncapped by the trigger of various stimuli, such as pH, temperature, light, ultrasounds and redox potential. Through surface modification, this system can be used for target delivery.

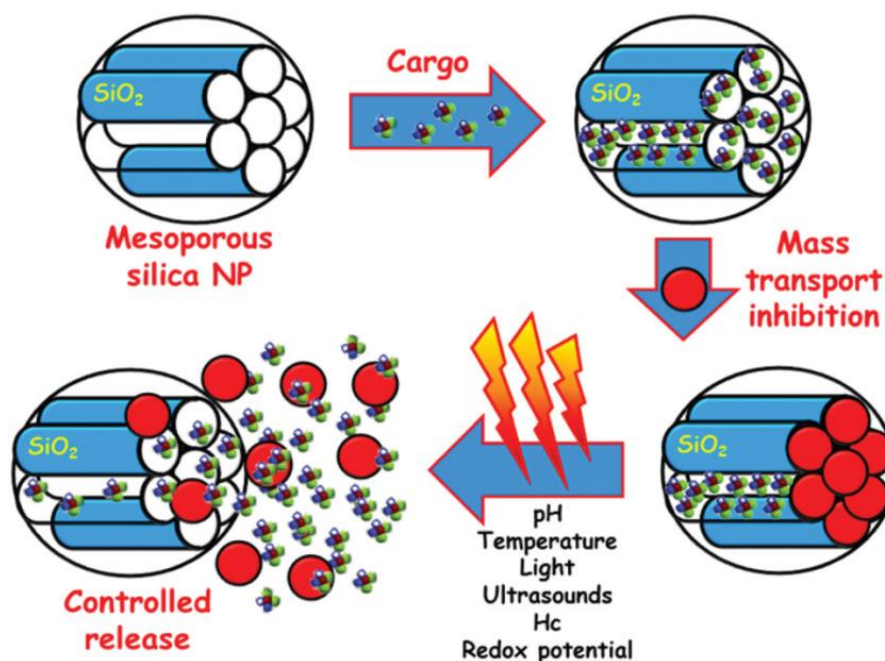


Figure 1: Typical approach for MSNs-based stimuli responsive drug delivery systems

(reprinted from Reference 14).

If the capping groups are sensitive to the unique stimuli of target cells or tissues, the system will be effective.¹⁴ Using the stimulus of pH, some research groups introduced the gatekeepers to the entrance of MSN pores by acid sensitive materials. For example, Au nanoparticles have been utilized as caps to avoid the premature cargo release. Au nanoparticles can cap the MSN pores through the formation of reversible boronate ester bonds²⁰ or acetal linkers,²¹ which could be hydrolyzed under acidic pH. With the aids of these pH sensitive bonds, the drug released could be controlled at certain location and time. Some other research groups used magnetic fields as external stimulus in drug delivery. For instance, Chen et al. have successfully capped MSNs with Fe₃O₄ nanoparticles (Figure 2).²² The MSNs were functionalized with 3-aminopropyltrimethoxysilane (APTS) and capped the pores through the amidation of the APTES with the 5.6 nm magnetic nanoparticles. Applying external magnetic fields, Fe₃O₄ particles were removed and resulted in fast drug release. Furthermore, the dual-responsive or multi-controlled drug delivery systems that respond to more than one stimulus have also been well developed recently.

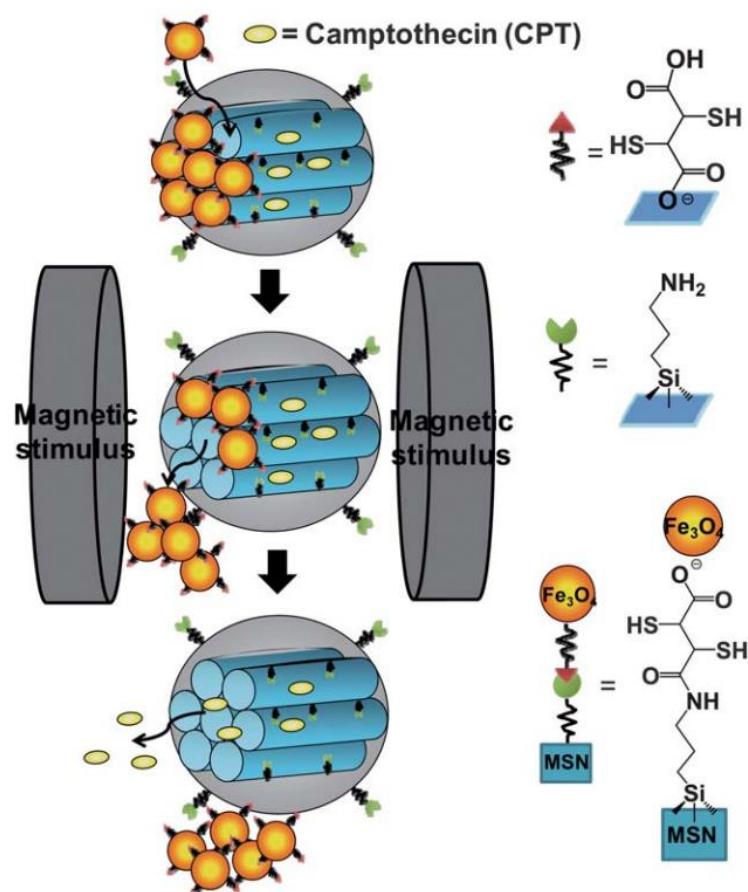


Figure 2: Scheme of the synthesis and structure of the Fe_3O_4 NPs-capped mesoporous silica drug nanocarriers (reprinted from Reference 22).

Liu et al. synthesized a multi-responsive drug delivery system by grafting β -cyclodextrin-bearing polymers to the MSNs through the disulphide bonds and blocked the pores by the formation of polymeric networks through the addition of diazo-linker.⁸ The obtained systems were responsive to the stimuli of UV light, α -cyclodextrin (α -CD is easier to react with azobenzene group than β -CD), and disulphide reductive agents including dithiothreitol (DTT).

However, these stimuli responsive drug delivery systems with gatekeepers have the

potential defect of burst release. Since the drugs are generally loaded by diffusion,²³ drugs interact with carriers by weak physical bonds. Once the gatekeeper is removed from the MSNs by stimuli triggers, the preloaded drugs will experience a rapid release from the carriers, which results in the quick rise of drug's blood concentration and momentarily plateaus. Generally, more than 80 % of loaded drugs are released within 6 h.^{5, 24, 25}

To overcome this problem, the drug delivery systems that using stimuli sensitive linkers to conjugate drugs to carriers covalently should be taken into consideration to achieve sustained drug release. Compare with the physically loading approaches, the sustained drug release is able to keep the concentration of anticancer drugs at a steady state level in order to prolong the effective concentration time of drugs and make the less frequency of drug administration, which will provide more benefits and be more efficient for modern cancer therapy.

2.3 Covalent conjugation of drugs to carriers by pH sensitive linkers

The use of pH to trigger drug release is based on the fact that the extracellular pH of tumor cells is lower than that of blood or healthy tissues. Normally, blood and healthy tissues have the neutral environment with a pH of around 7.4, while for some tumor cells, the extracellular pH can decrease to around 5.0.²⁶⁻²⁸ In order to establish successful pH responsive drug delivery systems to cancer cells, the conjugated linkers between drugs

and carriers should be stable at the microenvironment of pH 7.4 and be able to be cleaved rapidly at acidic micro environment to release the loaded drugs. With consideration of the structure and functional groups of a model anticancer drug of doxorubicin, the drugs can be conjugated to the surface of mesoporous silica nanoparticles by a variety of linkers to form different pH responsive bonds, which ranges from amide bonds to hydrazone bonds.

2.3.1 Amide bonds

The amide bond or peptide bonds is the covalent bond with the chemical formula -C(O)-NH-. It can be formed by the reaction of carboxyl groups and amino groups as shown in Figure 3 through 1-ethyl-3-(3-dimethylaminopropyl) carbodiimide (EDC) chemistry. In order to form the acid labile amide bonds, the drug carriers are required to be modified to the presence of surface carboxyl groups so as to react with the amino groups of DOX. In order to improve the yield, N-Hydroxysuccinimide (NHS) molecules are always used to active the carboxylic groups before the EDC coupling reaction.

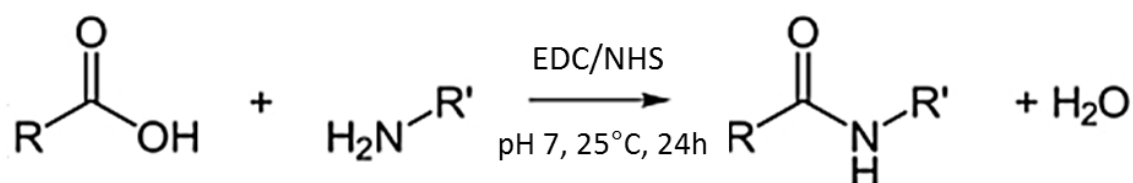


Figure 3: EDC coupling reaction in the presence of NHS.

Among varieties of acidic sensitive linkers, cis-aconitic anhydride is widely used to conjugate DOX to carriers.²⁹⁻³¹ Using EDC as the carboxyl activating agent, the carboxyl groups on cis-aconitic anhydride will couple with the primary amines on DOX to yield amide bonds. Recently, Yabbarov and co-workers synthesized a three-component drug delivery system, which included recombinant third domain of alpha-fetoprotein (rAFP3D) as targeting vector, polyamidoamine (PAMAM) generation 2 (G2) dendrimer and anticancer drug of DOX for cancer therapy (Figure 4).²⁹ The dendrimers are used to increase the number of chemical groups and drug loading. Through the linker of cis-aconitic anhydride, DOX was conjugated to the dendrimers covalently, and the resulting amide bonds were relatively stable at the physiological environment of pH 7.4, with 8 % DOX released for 24 hours. However, at pH 5.5, the hydrolysis of amide bonds could lead to the release of preloaded DOX drug.

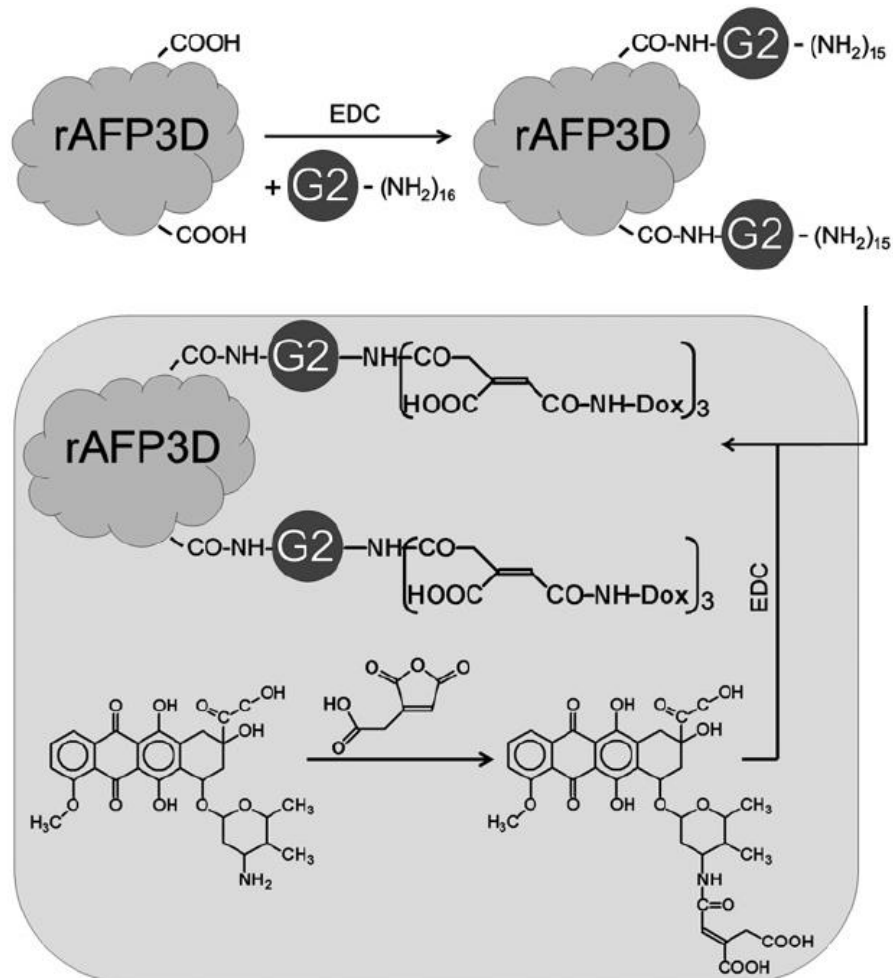


Figure 4: Scheme of conjugate synthesis of rAFP3D-G2-Dox

(adapted from Reference 29).

In addition, Du et al. utilized the acid labile linker of cis-aconitic anhydride to conjugate DOX with the folate-bovine serum albumin (BSA), and then attached folic acid to improve targeting ability.³¹ BSA is a biocompatible protein based drug delivery carrier containing 30 to 50 amino groups. After the conjugation, the synthesized particles could well disperse in water with an average size of 20 nm. In their report, the DOX release rate at pH 5.5 was 5 fold higher than that at pH 7.2, and the system had obvious

advantages of biodegradability, biocompatibility, and low toxicity to normal tissues. Furthermore, Lavignac et al. developed another strategy to conjugate DOX to the amino pendant groups of poly(amidoamine) (PAA) via the cis-aconitic anhydride linker associated with a loading capability of 28-35 μg of drugs per mg carriers.³⁰ Due to the cleavage of amide bonds, at low pH, up to 35 % of loaded DOX could be released.

However, the systems using the acid sensitive cis-aconitic anhydride linkers have the common problem of poorly controlled released rates. Although the drug release is pH dependent, 80 % of cumulative drug release can be obtained around 6 hours, which is too fast for the sustainable release processes and may affect therapeutic efficacy.

2.3.2 Hydrazone bond

Hydrazone bond is the functional group with chemical structure of $-\text{C}=\text{NNH}-$. It can be formed by the reaction of ketones or aldehydes with amines. The mechanism of its formation is shown in Figure 5, where the ketonic group is from DOX, while hydrazine group is from the carriers. The formed hydrazone linkers are stable at neutral pH environment, whereas at a low pH condition, its cleavage can accelerate drug release.^{32, 33}

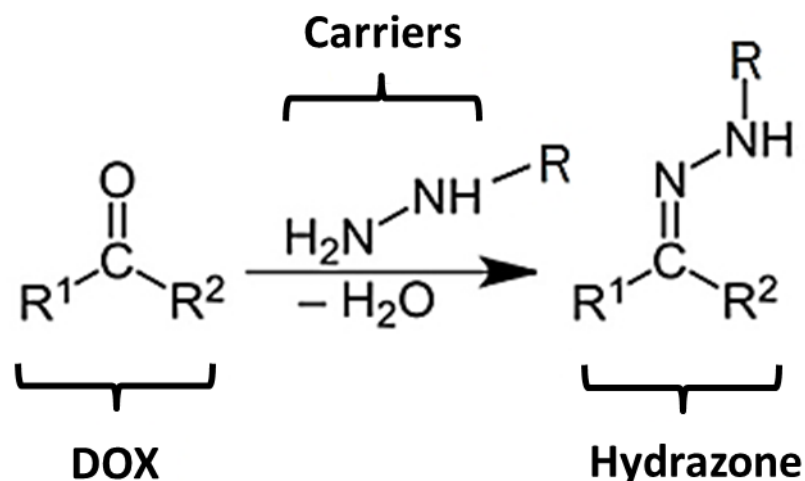


Figure 5: Reaction for hydrazone formation

Fan and co-workers reported a method to synthesize the target drug delivery system using 180 nm MSNs as the carriers (Figure 6).³⁴ The anticancer drug DOX was covalently conjugated to the MSNs by the carboxylic hydrazone linker which is acid cleavable. In order to achieve active targeting delivery, folic acid was conjugated to the MSN. In their study, the amine functionalized MSNs was first synthesized by introducing 3-aminopropyl -trimethoxysilane. The targeting agent of folic acid was conjugated to the MSNs through the amidation reaction, and DOX was incorporated into the functionalized MSNs through the formation of hydrazone bonds.

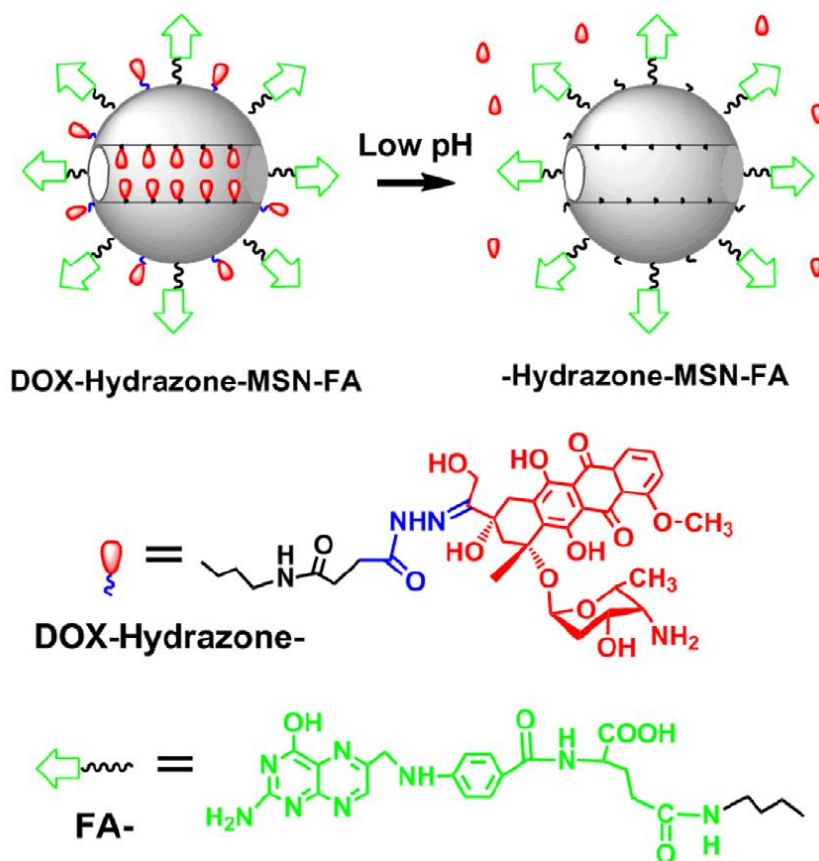


Figure 6: Synthesis of MSNs based targeted prodrug system with hydrazone linker
(adapted from Reference 34).

Following this strategy, the premature release of DOX could be controlled to less than 10% at pH 7.4 to minimize DOX's side effects, while in an acidic environment with pH 6.0, the release of DOX was governed by the hydrolysis of hydrazone linkage. The main defect of this approach was its low drug release rate. From their results, at pH 6.0, the accumulated release of DOX was less than 50 % within 72 hours, which might affect the effectiveness of cancer treatment.

Recently, She et al. have developed a new pH sensitive drug delivery system based on dendronized heparin-DOX conjugate nanoparticles.¹⁰ Heparin is a biodegradable and

non-cytotoxic polysaccharide, and it has been widely used as an anticoagulant drug and the anticancer drug delivery carrier. In their work, the peptide dendrons were covalently linked to heparin via click reaction to form the 'dendronized polymer'. The anticancer drug DOX was then conjugated to dendrons through the acid-labile hydrazone bond by the reaction of ketonic groups and hydrazine groups. Due to the features of DOX and heparin, the system would convert to nanoparticles by self-assembly, where the hydrophobic DOX forms the inner cores and hydrophilic heparin forms shell layers. At pH 7.4, less than 20 % of DOX were released from the nanoparticles after 56 hours, while at pH 5.0, because of the cleavage of hydrazone bonds, more than 80 % drug released was achieved. This system has the ability to control the release of loaded anticancer drugs at acidic microenvironment.

In addition, some other strategies using hydrazone bonds to govern the pH dependent DOX release have also been investigated. Kaminskis et al. reported a system using 4-(hydrazinosulfonyl) benzoic acid (HSBA) linker to graft DOX to the carrier of PEGylated polylysine dendrimers.¹¹ Besides the advantages of extended circulation time, biodegradability, and preferential tumor targeting, the HSBA hydrazone linker showed good stability over 72 hours at physiological pH, and released approximately 100 % of loaded drug within 24 hours at acidic environment. Aryal et al. successfully immobilized doxorubicin to gold nanoparticles by hydrazine modified methyl thioglycolate (MTG) linker to synthesize the water-soluble and pH-responsive drug nanocarriers for cancer treatment.³⁵ In another study, Wu et al. developed a system using high molecular weight

gelatin drug as carriers (Figure 7).³⁶ DOX was conjugated to gelatin by hydrazone bonds and the glycylglycine linker took the advantages of biodegradability, low cytotoxic and pH depended release.

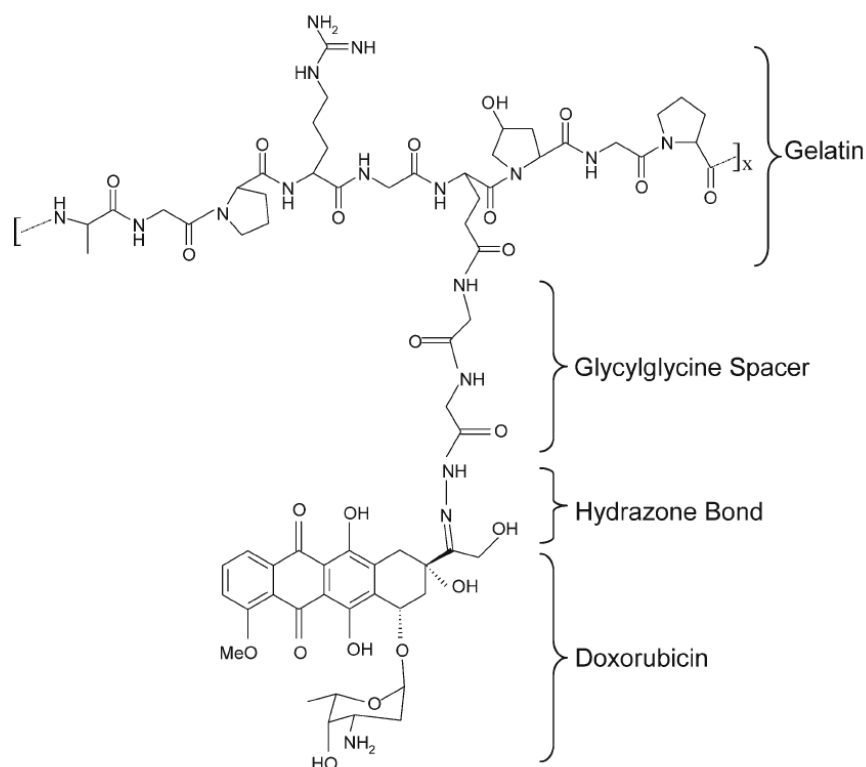


Figure 7: Structure of gelatin-DOX conjugates (G-DOX) (reprinted from Reference 36).

2.4 Drug conjugation by intracellular microenvironment responsive linker

Nowadays, intracellular biomolecules are getting increasing interest as the stimuli to trigger drug release because of their biological activities as well as outstanding biorecognition and catalytic ability. The synthesized intracellular micro-environment

responsive carriers can be used to delivery drugs with high specificity.³⁷ In this drug delivery system, drug carrier is conjugated with drugs by a “smart” linker, and triggers the release of cargos by the biocatalytic reaction of specific biomolecules. Among different kinds of intracellular biomolecules, enzyme or reducing agent are widely used as the stimuli to construct the enzyme and redox responsive drug delivery systems due to the increased presence of certain enzymes or reducing agents in cancer cells than normal tissues.

2.4.1 Enzyme responsive drug delivery systems

Generally, in a typical enzyme sensitive drug delivery system, the carriers are synthesized by degradable polymeric materials^{38, 39}, self-assembled nanospheres drug encapsulation⁴⁰, or inorganic nanoparticles^{41, 42} with surface modified molecules that are responsive to the presence of enzymes (Figure 8).

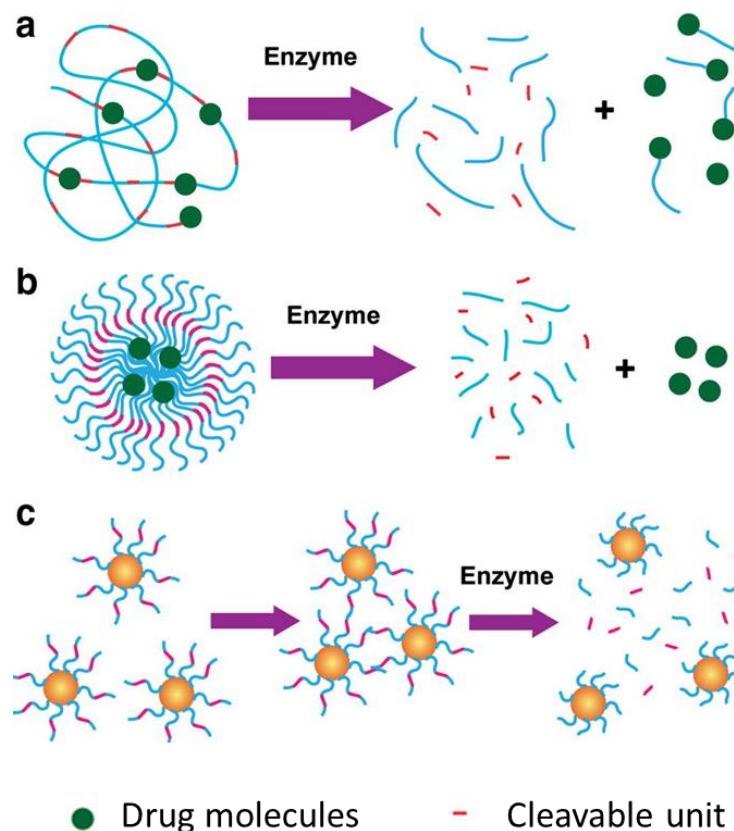


Figure 8: Enzyme responsive delivery: a) biodegradable polymers; b) self-assembled nanospheres; c) inorganic nanoparticles (adapted from Reference 23).

In order to improve specificity, the enzymes used should be over-expressed or activated only in unhealthy tissues, and they can be further classified into different categories such as proteases, lipases, glycosidases and oxidoreductases.²³

To date, some studies on enzyme-responsive systems have been carried out and their reported results are promising. Aromatic azo-linkers were used to conjugate anticancer DOX to generation 5 (G5) poly(amidoamine) dendrimers as reported by Medina and co-workers (Figure 9).⁴³ Aromatic azo-linkers could be cleaved by the enzyme of azoreductase existed especially in hepatic cells, resulting in the controlled and selective

release of DOX. Mechanistic study indicated that azoreductase enzyme activates the reduction of azobenzenes by the donation of a pair of electrons to the azo-bond from NADPH. The azo-bonds converted to the unstable hydrazo intermediates followed by reducing into its respective amines. The same team also modified the G5 dendrimers with polyethylene glycol (PEG) to improve its biocompatibility. As a result, in the absence of azoreductase enzyme, the release of DOX was controlled at less than 16 %, while in the presence of enzyme, more than 80 % of drugs were released within 4 hours.

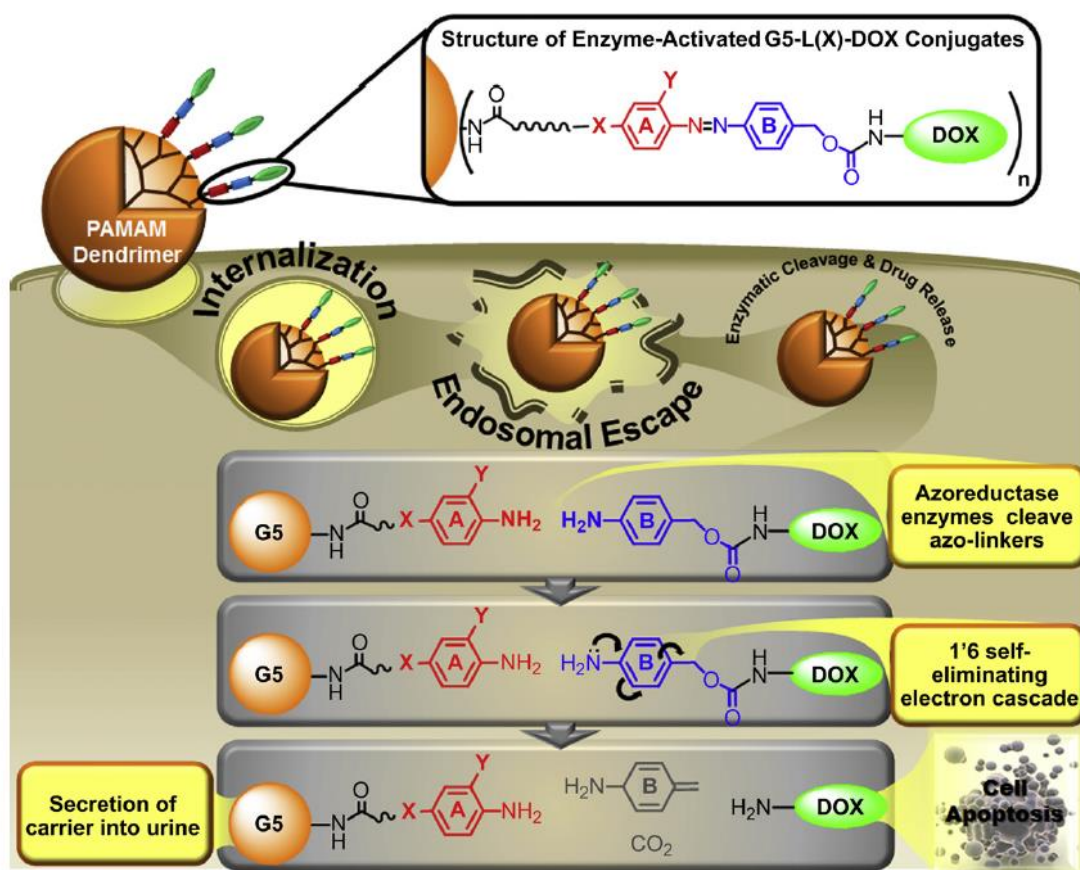


Figure 9: Scheme for the structure of G5-DOX conjugates and drug release by the reduction of azobenzenes (reprinted from Reference 43).

Besides, due to the high cathepsin B expression in tumor cells, Yang et al. developed the enzyme sensitive magnetic nanoparticles for intracellular-responsive drug delivery.⁴⁴ DOX was conjugated to the surfaces of silica magnetic carriers via a para-amino-benzyloxycarbonyl (PABC) linker and combined with the peptide precursors whose dipeptide sequence of H-Phe-Lys-OH could be cleaved by cathepsin B. The synthesized system exhibited the selective control intracellular release of the loaded drug when being treated with cathepsin B, leading to the potential of targeting drug delivery in the cells where this specific enzymes were highly expressed. In addition, by applying the same biocatalytic reaction mechanism, Dubowchik et al. used a self-immolative p-aminobenzyloxycarbonyl (PABC) linker to attach DOX to the internalizing monoclonal antibodies (MAbs), and the formed peptide bonds could be cleaved by cathepsin B. In their study, the conjugates presented up to 95 % of loaded drug release in rat liver lysosomes, but excellent stability in cytoplasm.⁴⁵

Moreover, in some cases, enzyme can activate the transformation of carriers to generate therapeutic molecules. For instance, utilizing the deamination of cytosine to uracil by cytosine deaminase, King et al. developed a system to convert nontoxic 5-fluorocytosine (5-FC) to the active antitumor drug 5-fluorouracil (5-FU).⁴⁶ The drug could accumulate in cancer cells 1000 times higher than normal tissues and inhibit 88–96 % tumor growth. Additionally, Hu et al. used nitroreductase, which has the ability to catalyze the reduction of nitro groups in a variety of substrates to produce relative hydroxylamine, as stimulus enzyme, and convert nitroaryl phosphoramides to cytotoxic phosphoramide drug by the

cleavage of benzylic C-O bonds.⁴⁷ The outstanding biological activity made the system become desirable for targeted delivery of toxic drugs to the hypoxic tumour cells.

2.4.2 Redox responsive drug delivery systems

The glutathione (GSH) is an intracellular biomolecule that has the redox potential and its concentrations in most cancer cells (8-10 mmol/L) are 2-10 times higher than that in normal cells (2-4 mmol/L) and 100-1000 times higher than in blood (1-2 $\mu\text{mol/L}$).^{48, 49} Therefore, the redox potentials between the reducing intracellular environment and oxidizing blood can be applied as a stimulus to activate the release of drugs from carriers, and different strategies have been developed to covalently conjugate drugs to carriers by redox responsive linkers.^{14, 50} Recently, most of the redox responsive drug delivery systems are developed by introducing disulfide linkages, which is labile to the reducing agent such as glutathione (GSH), dithiothreitol (DTT) or mercaptoethanol (ME), to control drug release.⁵¹

Li et al. developed a novel redox responsive drug delivery system. They loaded drug molecules to the carriers of mesoporous silica nanoparticles by physical interaction, and then coated the surfaces of mesoporous silica nanoparticles by poly(acrylic acid) (PAA) through disulfide linkers (Figure 10). The *in vitro* drug release showed that in the presence of 2 mM glutathione, the drug release could reach 49.4 %. In contrast, without glutathione, the total drug release was only 16.9 %. Their results clearly indicated that glutathione could effectively degrade the disulfide bonds and destroy the

cross-linked PAA networks to release the loaded drugs in the pores of mesoporous silica nanoparticles. However, the drug delivery system gave rise to burst release, where almost all drugs were released within 4 h.⁵²

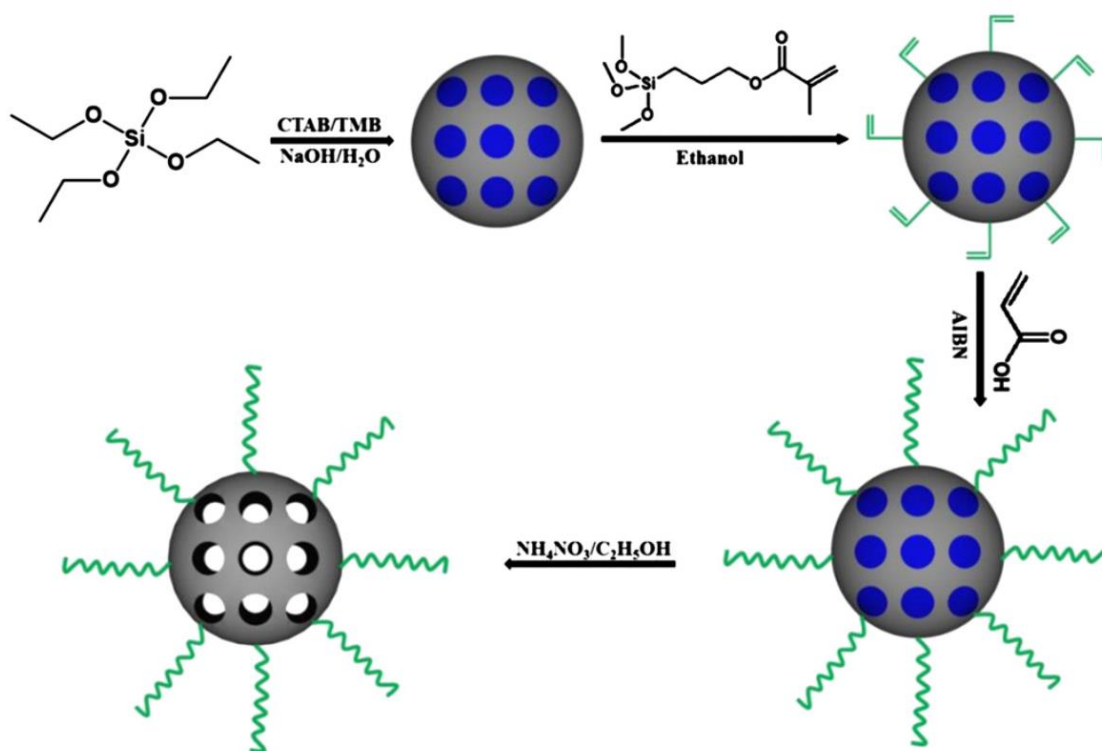


Figure 10: Schematic preparation process of PAA-MSNs (reprinted from Reference 52).

Other researchers have used disulfide bonds to conjugate drug molecules to other carriers. Tang et al. synthesized 130 nm to 150 nm mesoporous silica nanoparticles with an average pore size of 2.79 nm, and modified the inner and outer surface of mesoporous silica microspheres with disulfide bonds to get the MSN-SH particles, and conjugated the other end of disulfide bond with DOX through β -mercaptoethylamine linkers.⁵³ Their results indicated that the disulfide bonds could be cleaved in glutathione, but showed good stability in the phosphate buffer saline of pH 7.4. Therefore, the DOX could be only

released inside cells and effectively prevent leakage in blood. In their case, drugs could experience a sustained release of around 10 hours.

Comparing the drug release performance, both of enzyme responsive drug delivery systems and redox responsive drug delivery systems showed outstanding ability in controlled drug release. Such systems are stable in plasma and blood circulation, but release anticancer drugs efficiently in tumor sites to inhibit their growth. However, as comparing the drug release profiles of these two systems, redox responsive systems using disulfide bonds as smart linkers seem to be more feasible to achieve sustainable drug release. In most enzyme responsive systems, 90 % of released drugs were observed during the first 4-5 h, and in some cases, the drug release period was less than 1 h. For the redox responsive systems with disulfide linkers, as conjugating drugs to the carriers covalently, the average drug release period could reach to 8-10 h, which is longer than that of enzyme sensitive systems. Therefore, in order to construct the desired intracellular micro-environment responsive drug delivery system for sustained release, disulfide bonds might be more suitable to be used as the smart linker for drug conjugation and controlled release.

2.5 Summary

Controlled drug delivery system is crucial for cancer treatment in order to reduce the side effects of anticancer drugs as well as to improve therapeutic efficiency. However, for traditional drug delivery approaches, the loaded drugs always experience burst release, which would result in the shortness of drug effective time. In order to improve delivery efficiency, novel drug delivery systems based on drug conjugated silica nanoparticles are considered to be investigated in the thesis. The drug molecules will be conjugated to silica nanoparticles covalently by different smart chemical linkers. Based on the above literature review, the acid labile hydrazone bonds and redox labile disulfide bonds seem to be more interesting to achieve controlled and sustained drug release, but the detailed applications using silica nanoparticle carriers have not reported. Therefore, in this thesis, two kinds of drug conjugated silica nanoparticles systems:

- (1) pH responsive drug delivery systems with hydrazone linkers, and
- (2) redox responsive drug delivery systems with disulfide linkers

will be developed with detailed results presented in Chapters 3 and 4.

References

1. Australian Institute of Health and Welfare 2014. *Cancer in Australia: an overview 2014. Cancer series No 90. Cat. no. CAN 88. Canberra: AIHW.*
2. Y. Xie, T. R. Bagby, M. Cohen and M. L. Forrest, *Expert Opinion Drug Delivery*, 2009, **6**, 785-792.
3. C. K. Kim and S. J. Lim, *Archives of Pharmacal Research*, 2002, **25**, 229-239.
4. H. S. Jung, D. S. Moon and J. K. Lee, *Journal of Nanomaterials*, 2012, **2012**, 1-8.
5. P. DeMuth, M. Hurley, C. Wu, S. Galanie, M. R. Zachariah and P. DeShong, *Microporous and Mesoporous Materials*, 2011, **141**, 128-134.
6. K. Kono, S. Nakashima, D. Kokuryo, I. Aoki, H. Shimomoto, S. Aoshima, K. Maruyama, E. Yuba, C. Kojima, A. Harada and Y. Ishizaka, *Biomaterials*, 2011, **32**, 1387-1395.
7. C. Loira-Pastoriza, J. Todoroff and R. Vanbever, *Advanced Drug Delivery Reviews*, 2014, **75**, 81-91.
8. R. Liu, Y. Zhang and P. Feng, *Journal of the American Chemical Society*, 2009, **131**, 15128-15129.
9. I. Slowing, J. L. Vivero-Escoto, C. W. Wu and V. S. Lin, *Advanced Drug Delivery Reviews*, 2008, **60**, 1278-1288.

10. W. She, N. Li, K. Luo, C. Guo, G. Wang, Y. Geng and Z. Gu, *Biomaterials*, 2013, **34**, 2252-2264.
11. L. M. Kaminskas, B. D. Kelly, V. M. McLeod, G. Sberna, D. J. Owen, B. J. Boyd and C. J. Porter, *Journal of Controlled Release*, 2011, **152**, 241-248.
12. T. Sun, Y. S. Zhang, B. Pang, D. C. Hyun, M. Yang and Y. Xia, *Angew Chem Int Ed Engl*, 2014, **53**, 12320-12364.
13. C. Lu, B. Li, N. Liu, G. Wu, H. Gao and J. Ma, *RSC Advances*, 2014, **4**, 50301-50311.
14. M. Colilla, B. González and M. Vallet-Regí *Biomaterials Science*, 2013, **1**, 114-134.
15. J. Allouche, M. Boissiere, C. Helary, J. Livage and T. Coradin, *Journal of Materials Chemistry*, 2006, **16**, 3120-3125.
16. K. Dormer, C. Seeney, K. Lewelling, G. Lian, D. Gibson and M. Johnson, *Biomaterials*, 2005, **26**, 2061-2072.
17. S. Radin, G. El-Bassyouni, E. J. Vresilovic, E. Schepers and P. Ducheyne, *Biomaterials*, 2005, **26**, 1043-1052.
18. A. Popat, J. Liu, G. Q. Lu and S. Z. Qiao, *Journal of Materials Chemistry*, 2012, **22**, 11173-11178.
19. V. Mamaeva, C. Sahlgren and M. Linden, *Advanced Drug Delivery Reviews*, 2013, **65**, 689-702.

20. E. Aznar, C. Coll, M. D. Marcos, R. Martinez-Manez, F. Sancenon, J. Soto, P. Amoros, J. Cano and E. Ruiz, *Chemistry*, 2009, **15**, 6877-6888.
21. R. Liu, Y. Zhang, X. Zhao, A. Agarwal, L. J. Mueller and P. Feng, *Journal of the American Chemical Society*, 2010, **132**, 1500-1501.
22. P. J. Chen, S. H. Hu, C. S. Hsiao, Y. Y. Chen, D. M. Liu and S. Y. Chen, *Journal of Materials Chemistry*, 2011, **21**, 2535-2543.
23. R. de la Rica, D. Aili and M. M. Stevens, *Advanced Drug Delivery Reviews*, 2012, **64**, 967-978.
24. C. H. Tsai, J. L. Vivero-Escoto, Slowing, II, I. J. Fang, B. G. Trewyn and V. S. Lin, *Biomaterials*, 2011, **32**, 6234-6244.
25. X. Mei, D. Chen, N. Li, Q. Xu, J. Ge, H. Li and J. Lu, *Microporous and Mesoporous Materials*, 2012, **152**, 16-24.
26. A. Thistlethwaite, D. Leeper, D. Moylan and R. Nerlinger, *Radiation Oncology Biology Physics*, 1985, **11**, 1647-1652.
27. M. Prabakaran, J. J. Grailer, S. Pilla, D. A. Steeber and S. Gong, *Biomaterials*, 2009, **30**, 5757-5766.
28. J. Z. Du, X. J. Du, C. Q. Mao and J. Wang, *Journal of the American Chemical Society*, 2011, **133**, 17560-17563.

29. N. G. Yabbarov, G. A. Posypanova, E. A. Vorontsov, S. I. Obydenny and E. S. Severin, *Journal of Controlled Release*, 2013, **168**, 135-141.
30. N. Lavignac, J. L. Nicholls, P. Ferruti and R. Duncan, *Macromolecular Bioscience*, 2009, **9**, 480-487.
31. C. Du, D. Deng, L. Shan, S. Wan, J. Cao, J. Tian, S. Achilefu and Y. Gu, *Biomaterials*, 2013, **34**, 3087-3097.
32. Y. Yu, C. K. Chen, W. C. Law, E. Weinheimer, S. Sengupta, P. N. Prasad and C. Cheng, *Biomacromolecules*, 2014, **15**, 524-532.
33. C. Wang, P. Lv, W. Wei, S. Tao, T. Hu, J. Yang and C. Meng, *Nanotechnology*, 2011, **22**, 415101-415108.
34. J. Fan, G. Fang, X. Wang, F. Zeng, Y. Xiang and S. Wu, *Nanotechnology*, 2011, **22**, 455102-455112.
35. S. Aryal, J. J. Grailer, S. Pilla, D. A. Steeber and S. Gong, *Journal of Materials Chemistry*, 2009, **19**, 7879-7884.
36. D. C. Wu, C. R. Cammarata, H. J. Park, B. T. Rhodes and C. M. Ofner, 3rd, *Pharmaceutical Research*, 2013, **30**, 2087-2096.
37. T. L. Andresen, D. H. Thompson and T. Kaasgaard, *Molecular Membrane Biology*, 2010, **27**, 353-363.

38. F. M. Veronese, O. Schiavon, G. Pasut, R. Mendichi, L. Andersson, A. Tsirk, J. Ford, G. Wu, S. Kneller, J. Davies and R. Duncan, *Bioconjugate Chemistry*, 2005, **16**, 775-784.
39. J. Patterson and J. A. Hubbell, *Biomaterials*, 2011, **32**, 1301-1310.
40. Y. Malam, M. Loizidou and A. M. Seifalian, *Trends in Pharmacological Sciences*, 2009, **30**, 592-599.
41. C. Burns, W. U. Spindel, S. Puckett and G. E. Pacey, *Talanta*, 2006, **69**, 873-876.
42. N. G. Khlebtsov, *Analytical Chemistry*, 2008, **80**, 6620-6625.
43. S. H. Medina, M. V. Chevliakov, G. Tiruchinapally, Y. Y. Durmaz, S. P. Kuruvilla and M. E. Elsayed, *Biomaterials*, 2013, **34**, 4655-4666.
44. Y. Yang, J. Aw, K. Chen, F. Liu, P. Padmanabhan, Y. Hou, Z. Cheng and B. Xing, *Chemistry, an Asian Journal*, 2011, **6**, 1381-1389.
45. G. M. Dubowchik, R. A. Firestone, L. Padilla, D. Willner, S. J. Hofstead, K. Mosure, J. O. Knipe, S. J. Lasch and P. A. Trail, *Bioconjugate Chemistry*, 2002, **13**, 855-869.
46. I. King, D. Bermudes, S. Lin, M. Belcourt, J. Pike, K. Troy, T. Le, M. Ittensohn, J. Mao, W. Lang, J. D. Runyan, X. Luo, Z. Li and L. M. Zheng, *Human Gene Therapy*, 2002, **13**, 1225-1233.
47. L. Hu, C. Yu, Y. Jiang, J. Han, Z. Li, P. Browne, P. R. Race, R. J. Knox, P. F. Searle and E. I. Hyde, *Journal of Medicinal Chemistry*, 2003, **46**, 4818-4821.

48. X. Du, B. Shi, Y. Tang, S. Dai and S. Z. Qiao, *Biomaterials*, 2014, **35**, 5580-5590.
49. H. Gong, Z. Xie, M. Liu, H. Zhu and H. Sun, *RSC Advances*, 2015, **5**, 59576-59582.
50. Y. Chang, K. Yang, P. Wei, S. Huang, Y. Pei, W. Zhao and Z. Pei, *Angew Chem Int Ed Engl*, 2014, **53**, 13126-13130.
51. Y. Cui, H. Dong, X. Cai, D. Wang and Y. Li, *ACS Applied Materials & Interfaces*, 2012, **4**, 3177-3183.
52. H. Li, J. Z. Zhang, Q. Tang, M. Du, J. Hu and D. Yang, *Materials Science & Engineering. C, Materials for Biological Applications*, 2013, **33**, 3426-3431.
53. Q. Q. Tang, L. Yuan, D. Yang and J. H. Hu, *Acta Chimica Sinica*, 2010, **68**, 1925-1929.

Chapter 3 Doxorubicin conjugated silica nanoparticles: A pH regulated delivery system for controlled and sustained drug release

Doxorubicin conjugated silica nanoparticles: A pH regulated delivery system for controlled and sustained drug release

Wanxia Zhao, Xiaolin Cui, Hu Zhang, Jingxiu Bi*, and Sheng Dai*

School of Chemical Engineering, The University of Adelaide, Adelaide SA 5005 Australia

* To whom corresponding should be addressed

email s.dai@adelaide.edu.au and jingxiu.bi@adelaide.edu.au.

Statement of Authorship

Title of Paper	Doxorubicin conjugated silica nanoparticles: A pH regulated delivery system for controlled and sustained drug release
Publication Status	<input type="checkbox"/> Published <input type="checkbox"/> Accepted for Publication <input checked="" type="checkbox"/> Submitted for Publication <input type="checkbox"/> Publication Style
Publication Details	Submitted to Journal of Materials Chemistry B.

Principal Author

Name of Principal Author (Candidate)	Wanxia Zhao		
Contribution to the Paper	Performed experiments, analysed results, interpreted data and wrote manuscript.		
Overall percentage (%)	85%		
Signature		Date	

Co-Author Contributions

By signing the Statement of Authorship, each author certifies that:

- i. the candidate's stated contribution to the publication is accurate (as detailed above);
- ii. permission is granted for the candidate to include the publication in the thesis; and
- iii. the sum of all co-author contributions is equal to 100% less the candidate's stated contribution.

Name of Co-Author	Xiaolin Cui		
Contribution to the Paper	Assisted in experiments.		
Signature		Date	

Name of Co-Author	Hu Zhang		
Contribution to the Paper	Assisted in writing manuscript.		
Signature		Date	

Name of Co-Author	Jingxiu Bi		
Contribution to the Paper	Supervised development of work.		
Signature		Date	

Name of Co-Author	Sheng Dai		
Contribution to the Paper	Supervised development of work and assisted in writing manuscript.		
Signature		Date	

Abstract

Controlled drug delivery is crucial in the modern chemotherapy for cancer treatment to reduce side effects of anticancer drugs and reduce medical treatment costs. For a traditional drug delivery system, drugs are loaded into various delivery carriers by physical interaction, which results in drug leakage and burst release after administration. In order to overcome these problems, we developed a pH regulated drug delivery system by chemically conjugating drug molecules to carriers to achieve controlled and sustained drug release. Silica nanoparticles were selected as a typical drug delivery carrier and modified with tert-butyl carbazate on their surface. The anticancer drug, doxorubicin (DOX), was covalently conjugated to the surface of silica nanoparticles via the formation of an acid labile hydrazone linker. Under the physiological pH, the drug delivery system presents good stability to prevent DOX leakage and release, while at an acidic environment of pH 5.0 (pH outside cancer cells), the conjugated drugs can be released sustainably due to hydrolysis of the pH sensitive hydrazone bonds. From *in vitro* cell cultures against Hela cells and HEK 293 cells, the loaded DOX can be released effectively to cancer cells, while its cytotoxicity to normal cells is minimized. The obtained results clearly indicate that DOX conjugated silica nanoparticles with acid labile hydrazone linkers are feasible to construct an advanced drug delivery system with a capability for controlled and sustained release.

Keywords: pH-sensitive cleavage, drug delivery, doxorubicin, silica nanoparticles, surface modification, hydrazone

3.1 Introduction

Nowadays, chemotherapy has been widely applied as a primary method in the treatment of different types of cancers. However, due to lack of specificity to cancer cells, chemotherapeutic cancer treatment needs to consume a high dosage of cytotoxic anticancer drugs, which always brings serious side effects to patients.^{1, 2} In order to overcome this problem, a variety of drug delivery systems have been developed. For an ideal delivery system, the pre-loaded drugs should only be delivered to target cancer cells without premature drug release. Most of the successful traditional drug delivery strategies are based on the concept of capsulation to prevent premature release.³⁻⁶ Despite of its benefits, the obvious disadvantages are the leakage during delivery and uncontrolled burst release. In the capsulation systems, drugs are loaded into carriers by weak physical bonds. When triggered by various stimuli, most of loaded drugs will be released within a short time, which rapidly changes the drug concentration in blood and shortens its effective duration.⁷ Therefore, the covalent conjugation of drugs to carriers has been taken into consideration to manipulate the drug release profiles. For such a system, anticancer drugs can be loaded to carriers through a smart linker and released by cleavage of the stimuli-responsive linker to achieve controlled drug release, which makes the drug delivery system more feasible in sustained release and thus provides more benefits in cancer chemotherapy than traditional delivery methods.⁸ To date, a myriad of carriers for drug/carrier conjugation systems have been explored, such as polymeric nanoparticles, liposomes, dendrimers and others.⁹⁻¹³ Although some of them have displayed excellent

controlled release profiles, the application using inorganic carriers are rarely reported. Among inorganic nanoparticles, silica nanoparticles (SNs) have received high attention in biological applications due to their excellent biocompatibility, uniform nanostructure and easily modified surfaces.^{3, 4, 14}

On the other hand, the smart linkers employed to conjugate drugs to carriers can be cleaved by different stimuli, such as temperature, light, enzyme, redox potential and magnetic field,¹⁴⁻¹⁷ and a pH regulated system is receiving special interest and it has been designed to effectively trigger drug release.⁵ The physiological pH of human blood and normal tissues is around 7.4, whereas the extracellular pH of some tumors is around 5.0.^{18,}

¹⁹ Because of this significant pH difference between normal tissues and tumors, pH sensitive delivery systems can be used to achieve drug release only in the cancer cells. As such, researches had been extensively conducted to develop pH-sensitive drug-carrier conjugation delivery systems. For example, the anticancer drug, doxorubicin (DOX), has been conjugated to polymeric carriers through cis-aconitic anhydride to form amide bonds.^{20, 21} In some other cases, the drug has been conjugated to the carriers by Schiff base formation.²² In their studies, a high amount of drugs could be loaded into the carriers and released effectively to target cells, but rapid drug release arose from the fast hydrolysis of these pH sensitive linkers, which made it hard to achieve sustained release. Therefore, it is vital to explore a more suitable linker for the drug-carrier conjugation delivery systems. Among different pH sensitive linkers, hydrazone bonds should be able to present better performance in controlled and sustained drug release due to its relative

stability in acidic circumstances.²³⁻²⁶

In this study, we developed a novel pH sensitive silica based drug-carrier conjugation delivery system with acid-labile hydrazone bonds. The surface of well-defined silica nanoparticles was modified with hydrazine group by tert-butyl carbazate, and a model anticancer drug of DOX was conjugated to the surface of silica nanoparticles by reacting the ketonic groups of DOX with the hydrazine moieties on the modified silica nanoparticle surface to form hydrazone bonds. The good stability of hydrazone bonds under a physiologic pH makes the drug-carrier conjugation delivery system stable in blood circulation and normal tissues without undesired drug leakage. Cleavage of the hydrazone bonds under an acidic condition renders the loaded drugs to be effectively delivered to target cells. Besides detailed synthesis and characterization of DOX conjugated silica nanoparticles, the pH dependent controlled drug release and cell uptake have been systematically evaluated.

3.2 Materials and Methods

3.2.1 Materials

Doxorubicin hydrochloride (DOX) was purchased from Beijing Huafeng United Technology Co., Ltd. Tetraethyl orthosilicate (TEOS), 3-aminopropyltriethoxysilane (APTES), toluene, succinic anhydride, tert-butyl carbazate, sulfo-N-hydroxysuccinimide (sulfo-NHS), 1-ethyl-3-(3-dimethylaminopropyl) carbodiimide hydrochloride (EDC)

and trifluoroacetic acid (TFA) were purchased from Sigma-Aldrich. Ammonia aqueous (30%) and N,N-dimethylformamide (DMF) were from VWR International Pty Ltd. Ethanol and dimethyl sulphoxide (DMSO) were from Chem-Supply. Phosphate buffered saline (PBS) solution (pH 7.4), Dulbecco's modified Eagle medium (DMEM), fetal bovine serum (FBS), penicillin streptomycin (PS), 3-(4,5-dimethylthiazol-2-yl)-2,5-diphenyltetrazolium bromide (MTT) reagent, LIVE/DEAD[®] viability/cytotoxicity kit (containing calcein-AM and ethidium homodimer-1), cell culture flasks and well plates were purchased from Life Technologies Australia Pty Ltd. All of the chemicals were of analytic grade and used directly without further purification. Water used was from a Milli-Q water purification system with a resistivity higher than 18.2 MΩ·cm.

3.2.2 Synthesis of silica nanoparticles

Silica nanoparticles (SNs) were synthesized by a modified St öber method.² 1.5 ml water and 2.5 ml ammonia aqueous were mixed with 50 ml anhydrous ethanol. The temperature of the mixture was maintained at 40 °C by a water bath. After 20 min, 1.5 ml TEOS was added to the solution quickly and stirred continuously at 40 °C for 12 h. After the reaction, white precipitates were obtained and purified by centrifugation at 6000 rpm for 15 min and washed with ethanol and water for 3 times. Finally, the obtained silica nanoparticles were dispersed in 10 ml ethanol by ultrasonic dispersion for further use.

3.2.3 Introduction of pH sensitive linker on the surface of silica nanoparticles

Silica nanoparticle surface modification was conducted based on literature with slight modification.²⁷ 0.1 g purified silica nanoparticles (SNs) were dispersed in 40 ml anhydrous toluene under nitrogen for 30 min. Then, 0.15 ml APTES was added to the mixture, followed by reflux at 110 °C for 16 h. After the reaction, the mixture was cooled down to room temperature, and the synthesized amine functionalized silica nanoparticles (SNs-NH₂) were washed by ethanol for 3 times and stored.

0.1 g SNs-NH₂ was dispersed in 15 ml DMF. 0.9 g succinic anhydride was dissolved in 5 ml DMF and added into the suspension of SNs-NH₂. After 6 h reaction at room temperature under vigorous stirring, the mixture was centrifuged and washed with water to get the carboxyl functionalized silica nanoparticles (SNs-COOH).

50 mg of SNs-COOH was dispersed in 20 ml DMF and reacted with 54 mg sulfo-NHS and 54 mg EDC for 45 min before adding 37 mg tert-butyl carbazate. The mixture was stirred at room temperature for another 16 h, and the white precipitate of Boc-hydrazine modified silica nanoparticles (Boc-hydrazine-SNs) was acquired by centrifuge at 6000 rpm for 15 min. The product was washed with ethanol and water to remove any unreacted residual.

Finally, 50 mg Boc-hydrazine-SNs was dispersed in 2 ml DMF and stirred at 550 rpm under room temperature, followed by adding 15 ml TFA to the suspension. The mixture was reacted for another 24 h. After centrifuging and washing with ethanol and water, the

hydrazine group modified silica nanoparticles (hydrazine-SNs) were obtained, and dispersed in 5 ml ethanol for further use.

3.2.4 Characterization

Scanning electron microscopy (SEM) images were taken on a Quanta 450 FEG environmental emission scanning electron microscopy at the operating voltage of 30 kV and work distance of 10 mm. Zeta potential and dynamic light scattering (DLS) measurements were carried out using a Malvern Zetasizer Nano ZS (ZEN 3600). Fourier transform infrared (FTIR) spectra were recorded using the Thermo Scientific Nicolet 6700 FTIR spectrophotometer at room temperature. UV-vis absorption spectra were obtained by a Shimadzu UV-Visible spectrophotometer (UV-1601), and the standard calibration curve (Figure S1) of DOX was established at a wavelength of 480 nm. The viability of cells was measured using an ELx808 Absorbance Microplate Reader from BioTek. Fluorescent emission and excitation images were recorded on a ZEISS Axion Vert.A1 inverted microscope. The live cells were viewed using green fluorescent port filter with excitation wavelength of 470 ± 20 nm and emission wavelength of 525 ± 25 nm, while the dead cells were viewed using DsRed filter with excitation wavelength of 545 ± 13 nm and emission wavelength of 605 ± 35 nm.

3.2.5 Drug loading and *ex vivo* doxorubicin release

2 mg doxorubicin hydrochloride was added in 1 ml PBS solution, and 20 mg of hydrazine-SNs were dispersed in 5 ml PBS solution. The doxorubicin hydrochloride solution was added into the hydrazine-SNs suspension followed by stirring at room temperature for 24 h in darkness. After washing the mixture with ethanol for 3 times to remove unreacted DOX, the red color solid products of DOX conjugated silica nanoparticles (DOX-hydrazone-SNs) were obtained. The unreacted DOX concentration in the supernatant of reaction mixture was examined by a UV-visible spectrophotometer at 480 nm, and the drug loading efficiency on silica nanoparticles was estimated using the following equation:

$$\begin{aligned} & \text{Drug loading efficiency (\%)} \\ &= \frac{\text{DOX weight in feed} - \text{unreacted DOX weight in the supernatant}}{\text{weight of silica nanoparticles}} \times 100\% \quad (1) \end{aligned}$$

To evaluate the *ex vivo* drug release behavior, 5 mg of DOX conjugated silica nanoparticles were dispersed in 10 ml PBS buffer solutions with different pH values of 5.0, 6.5 and 7.4. The mixtures were stirred at 37 °C in darkness. For analyzing the amount of released DOX from nanoparticles, 1 ml aliquot was removed from the mixture at 5 h, 8 h, 12 h, 16 h and 24 h and then equivalent volume of fresh PBS solutions were added. The concentration of released DOX was examined by a UV-visible spectrophotometer at 480 nm. All drug release evaluations were conducted in triplicate for each sample.

3.2.6 Cytotoxicity

The cytotoxicity of silica nanoparticles with and without DOX conjugation was conducted against human cervical cancer HeLa cells and human embryonic kidney HEK 293 cells. Both cells were incubated in plastic flasks with DMEM cell culture medium containing 1 % PS and 10 % FBS at 37 °C with 5 % CO₂. The MTT assay analysis was then applied to evaluate cell viability. Cells were seeded in a 96-well plate at a density of 5.0×10^4 cells/well with 150 µl growth medium. After incubation for 24 h, the growth medium was replaced by 150 µl fresh one which contained 11 µl sample of silica nanoparticles, DOX conjugated particles or free DOX. The equivalent concentration of DOX in the samples ranged from 0 to 1.25 µg/ml and repeated in 4 wells. After another 24 h incubation, 10 µl MTT was added, and after another 4 h, the growth medium of each well was removed and 150 µl DMSO was added. The absorbance was measured by a microplate reader at a wavelength of 595 nm, and the cell viability was presented as percentage based on the untreated cells.

3.2.7 Fluorescence Imaging Analysis

HeLa cells and HEK 293 cells were seeded into a 24-well plate at the density of 2.5×10^5 cells/well with 1 ml growth medium. After incubation for 24 h, the growth medium was replaced with the fresh one and 0.1 ml of DOX conjugated silica nanoparticles at a concentration of 100 µg/ml in PBS solution were added. With further 2 h, 8 h, 16 h and 24 h incubation, the fluorescence microscopic analysis was conducted. After washing with

PBS solution thrice to remove growth medium, the cells were treated with 400 μl of fluorescence staining reagent, which contained 2 μM calcein-AM and 4 μM ethidium homodimer-1, for 30 min. The fluorescence images were obtained and analyzed using a fluorescence microscope, where calcein was excited at 488 nm while ethidium homodimer-1 at 530 nm.

3.3 Results and Discussion

3.3.1 Synthesis of hydrazine-silica nanoparticles and characterization of surface functional groups

The hydrazine-silica nanoparticles are synthesized as the drug carriers by the method given in Figure 1. When exploring nanoparticle application in drug delivery, suitable size and uniform structure, the key important factors, need to be considered, which can be tailored by varying precursor feed molar ratios, reaction temperatures and reaction times. The particle sizes of silica nanoparticles (SNs) were analysed by SEM and dynamic light scattering (DLS). According to the SEM image in Figure 2B, the synthesized silica nanoparticles are monodispersed with a mean diameter of around 180 nm, which is close to the hydrodynamic diameter obtained from DLS. For nanoparticle-based drug carriers, large sized particles will affect cell uptake and accumulation ability by reducing the permeability and retention (EPR) effect.^{28, 29} On the other hand, when the particles are less than 100 nm, it may cause cytotoxicity.³⁰ Therefore, the silica nanoparticles with a

size of 180 nm are considered to be suitable for the drug delivery purpose. The polydispersity index (PDI) of the silica nanoparticles from DLS is 0.012, indicating that the size distribution is narrow and the particle dispersity is uniform. The hydrodynamic particle size from DLS after pH sensitive linker surface modification (hydrazine-SNs) is found to be 295 nm. The increase in particle size is mainly due to the significant hydration of various functionalization groups on the silica nanoparticle surfaces. No aggregation of silica nanoparticles is observed after surface modifications.

For the details of surface modification, the silica nanoparticles were first modified with amino groups. Silica nanoparticles and 3-aminopropyltriethoxysilane (APTES) were reflux in toluene at 110 °C under nitrogen protection to avoid the hydrolysis of APTES by water. Conductometric titration was used to quantify the amino groups on silica nanoparticle surfaces, and it was found to be 0.648 mmol $-NH_2$ per gram of silica nanoparticles (Figure S2). After that, succinic anhydride was charged to introduce carboxyl groups on the SNs- NH_2 surface. Excess amount of succinic anhydride was used to prevent possible crosslinking, and the feed molar ratio of succinic anhydride to the amino groups on the silica nanoparticles surface was kept at 5:1. In the next step, the carboxyl groups on the silica nanoparticle surface were reacted with the amino groups of tert-butyl carbazate by forming amide bonds via EDC coupling. After removing the amino protection groups by TFA, the exposed hydrazine bonds were used to conjugate doxorubicin, and the resulting hydrazone bonds between silica nanoparticles and DOX is pH sensitive. During all these synthesis steps, product purification was easily handled by

using centrifugation at 6000 rpm for 15 min.

To confirm the introduction of various functional groups on the silica nanoparticle surface, zeta potential measurements were carried out with results shown in Figure 3. The silica nanoparticles before any surface modification have a negative zeta potential value of around -30.5 mV due to hydrolysis of the surface OH groups. After APTES modification, the zeta potential changes to +26.8 mV, which indicates the presence of excess positively charged amino groups on the surface of SNs. After reaction with succinic anhydride, the negatively charged carboxyl groups give rise to a zeta potential of -14.4 mV. The further reaction with tert-butyl carbazate shifts the zeta potential back to be positive again (around +30 mV) due to the introduction of amino groups on the SN surface. The zeta potential study clearly indicates that each step for modification of surface functional groups is successful, and the pH sensitive linker has been conjugated to the surface of silica nanoparticles. Moreover, it is also evident that all absolute modified zeta potential values are above 15 mV, which implies good stability of SNs in the aqueous system.

Furthermore, the FTIR spectra shown in Figure 4 are also able to provide confirmation on successful surface modifications. After amino group functionalization, a new peak at 1450 cm^{-1} is due to the vibration of N-H bending. Compared with SNs and SNs-NH₂, carboxyl functionalized SNs show new peaks at 1550 and 1710 cm^{-1} , which are assigned to the stretching vibration of amide groups and carboxyl groups, respectively. At the same time, the N-H bending peak becomes weaker since some of the amino groups on the

surface have been reacted with succinic anhydride. After further conjugating the pH sensitive linker, a new vibration peak at 1725 cm^{-1} is observed due to the vibration of -CO-O- on the amino protection groups. For the hydrazine-SNs, the absorption band of -CO-O- disappears and the peak at 1369 cm^{-1} associated with the structure of the secondary amine in hydrazine groups is evident. Obviously, FTIR spectra further suggest the success of various surface modifications on silica nanoparticles.

3.3.2 Loading DOX to hydrazine-silica nanoparticles by covalent bonds

Doxorubicin was conjugated to the silica nanoparticles by formation of hydrazone linkers.¹⁸ In this case, the hydrazine groups on the surface of silica nanoparticles react with the ketonic groups of DOX to form pH-sensitive hydrazone bonds. After DOX conjugation, the color of hydrazine-SNs changes from white to red. In the FTIR (Figure 4), the attachment of DOX to silica nanoparticles contributes to a new stretching vibration bond at 1726 cm^{-1} .

3.3.3 pH responsive *ex vivo* DOX release

The physiological pH in the human blood and healthy tissues is around 7.4, while the extracellular pH of tumor cells is lower. For some tumors, the extracellular pH can decrease to around 5.0. Taking this into consideration, the above prepared drug carrier conjugate system may be used to selectively deliver drugs to tumors. The release ability of DOX was first *ex vivo* examined in the PBS buffer solutions at three different pHs (5.0,

6.5 and 7.4), where pH 7.4 is used to simulate the physiological condition, pH 6.5 and 5.0 are used to simulate the extracellular conditions of different tumors. The amount of DOX released to the buffer solutions was qualified by a UV-visible spectroscopy at 480 nm. The detailed pH dependent DOX released profiles are presented in Figure 5. Under the physiological pH, less than 10 % of loaded DOX can be released within 24 h, whereas significant increases in drug release are observed at low pHs due to the instability of hydrazone bonds in an acidic environment. At pH 5.0, approximate 55 % of loaded DOX are released from silica nanoparticles within 24 h, while at pH 6.5, the drug release amount is about 45 %. Comparing with the release profiles between pH 5.0 and pH 6.5, a lower pH facilitates rapid drug release. This difference is attributed to the rapid cleavage of hydrazone linkers at a lower pH, and more acidic conditions accelerate its degradation to enhance DOX release. As a result, the hydrazone linkers have good stability at the physiological pH, which means our drug delivery system is able to minimize the leakage and release of anticancer drugs in the normal tissues and reduce chemotherapeutic side effects. However, rapid cleavage of hydrazone bonds at the acidic environment makes this system release drugs to tumor cells. The accumulated drugs in cancer cells will inhibit the growth of tumours and enhance the therapeutic efficacy synergistically.

pH responsive drug delivery systems have been studied by other researchers.^{5, 22, 31} They have conjugated DOX to various carriers using different pH sensitive linkers to ensure drugs to be released at the desired pH. Yabbarov *et al.* conjugated DOX to the surface of dendrimers covalently using the linker of cis-aconitic anhydride.²⁰ The formed amide

bond was stable at the physiological pH, and the hydrolysis of amides at a low pH led to the release of loaded drugs. In their case, 80 % of loaded drugs were released within 6 h, which was too fast for the sustainable release. In our study, we utilize hydrazone bonds to conjugate drugs to silica nanoparticles, which is relatively stable in acidic conditions than amide bonds. The loaded DOX can be slowly and continuously released within 24 h. This sustained drug release profile will keep the concentration of anticancer drugs at a steady level over a prolonged effective time range and minimize the frequency of drug administration. Obviously, such a drug delivery system will be more feasible for the application in controlled and sustained drug release than that being recently reported.²⁰⁻²²

3.3.4 Cytotoxic evaluation against Hela cells and HEK 293 cells

The cytotoxicity experiments of hydrazine-SNs, DOX-hydrazone-SNs, and free DOX against Hela cells (cancer cells) and HEK 293 cells (normal cells) for 24 h were conducted with the MTT assay. As shown in Figure 6, free DOX has the highest cytotoxicity to both cancer cells and normal cells, whereas hydrazine-SNs present low cytotoxicity to both cell lines. Incubating at a high concentration of 100 µg/ml of hydrazine-SNs for 24 h, the cell viability is more than 85 %, which means hydrazine-SNs have good biocompatibility and it is safe to be used as drug delivery carriers. However, after incubating with DOX conjugated silica nanoparticles, when increasing the equivalent concentration of DOX to 1.25 µg/ml (equal to 100 µg/ml DOX-hydrazone-SNs), around 50 % decrease in cell viability can be observed in Hela

cells, and the decrease is much sharper than that in HEK 293 cells. In addition, the cell viability of HeLa cells after incubating with DOX-hydrazone-SNs becomes closer to the cell viability after incubating with free DOX. At the highest concentration of 100 µg/ml, the cell viability difference between DOX-hydrazone-SNs and free DOX reaches 40 % for HEK 293 cells, while the difference for HeLa cells is only 15 %.

Cell viability decrease is caused by the cytotoxicity of DOX. The low pH environment for HeLa cells can trigger cleavage of the hydrazone bonds. When incubating HeLa cells with DOX-hydrazone-SNs, its low extracellular pH causes the conjugated DOX to be released from the surface of silica nanoparticles. The higher concentration of DOX-hydrazone-SNs presents in the growth medium, the more drugs can be released and lower cell viability can be observed. In contrast, since HEK 293 cells cannot provide an acidic extracellular environment, the hydrazone bond is relative stable in this condition, and thus only a small amount of DOX is released from the surface of silica nanoparticles. Even increasing the concentration of DOX-hydrazone-SNs, the cell viability for HEK 293 cells still displays no significant difference. As such, our drug delivery system has the ability to control the drug release in tumors cells, but minimize side effects of DOX to normal cells.

3.3.5 Cell uptake analysis by live/dead cell assays

To further demonstrate the effectiveness of DOX-hydrazone-SNs in tumor cells, the fluorescence microscopic images were taken to visualize the cell viability and drug uptake

behaviors. HeLa cells and HEK 293 cells were treated with DOX conjugated silica nanoparticles for 2 h, 8 h, 16 h and 24 h respectively, and the mixture of live and dead cells were separately stained with calcein-AM and ethidium homodimer-1 dyes. The esterase in the live cells generates calcein by removing the AM groups from Calcein-AM to emit green fluorescence, while ethidium homodimer-1 intercalates with the DNA of dead cells through the damaged areas on their membrane and emits red fluorescence. As a result, the cell viability can be visually verified by the intensity of fluorescence, where green fluorescence indicates the population of live cells and red one indicates the population of dead cells. From Figure 7, after 2 h incubation, only a few red fluorescence can be observed in HeLa cells, which means most of cells are still alive. However, with further incubation, especially after 8 h, the intensity of red fluorescence apparently increases, and after 24 h, the intensity of red fluorescence and green fluorescence are almost same, which means the cell viability of HeLa cells has decreased to about 50 %. This result indicates that the DOX has been efficiently released to cancer cells and the minor red fluorescence increase in the first 8 h means the drug is sustainably released. On the other hand, for the HEK 293 cells, as the incubation time extends, the intensity of red fluorescence just presents a slight increase, even after 24 h, the cell viability still remains around 70-80 %, which means DOX is difficult to be released to normal cells since its neutral extracellular pH cannot trigger the release of drugs. Therefore, the *in vitro* study clearly confirms the drugs being conjugated on the SN surface can be successfully released to cancer cells but the drug toxicity to normal cells is minimized.

3.4 Conclusions

In summary, we have successfully modified the surface of silica nanoparticles with hydrazine functional groups and developed a pH responsive drug conjugation delivery system using doxorubicin as a model anticancer drug. The silica nanoparticles synthesized has a uniform size of around 180 nm, and conjugate with DOX covalently through formation of the hydrazone bonds. The *ex vivo* drug release results show the drug release system presents good stability under physiological pH, but sustained pH-dependent release behavior under a weak acidic environment due to cleavage of the pH sensitive hydrazone bonds. Based on the *in vitro* cytotoxicity evaluation, the delivery carrier (hydrazine-SNs) shows good biocompatibility, and the drug conjugated delivery system can effectively release loaded drugs to cancer cells rather than normal cells. That is also evidenced from the live/dead cell assay. Therefore, our pH responsive drug delivery system using the hydrazone linkers is able to achieve controlled and sustained drug release, which makes it more feasible in the application of future cancer treatment.

Acknowledgement

This work was financially supported by the Australian Research Council (ARC) Discovery Projects (DP140104062 and DP110102877).

Supporting Information Available

The calibration curve of DOX and the potentiometric/conductometric titration of SNs-NH₂ are available in supporting information.

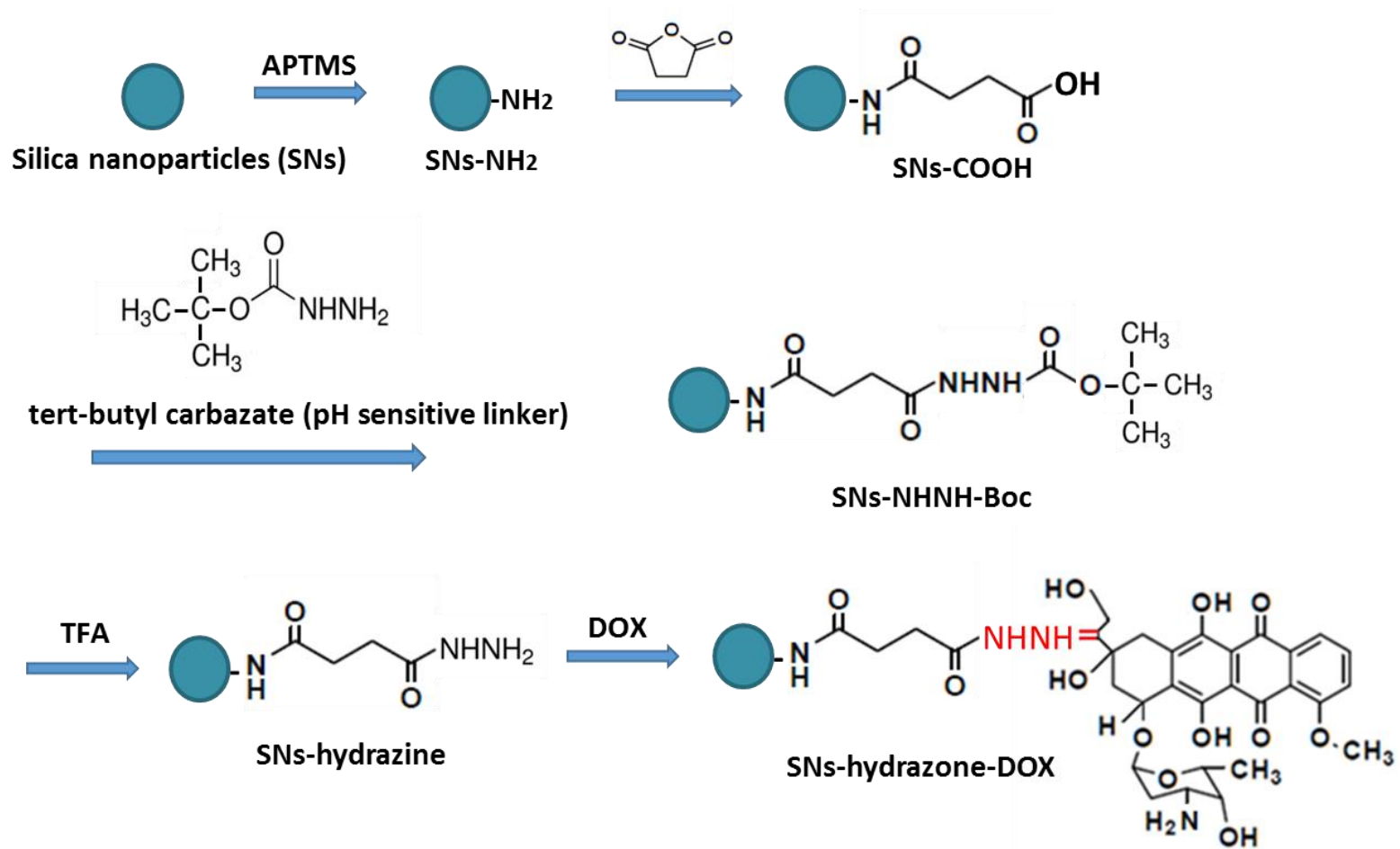


Figure 1: Synthesis scheme of pH sensitive linker modified silica nanoparticles with anticancer drug (DOX) loading.

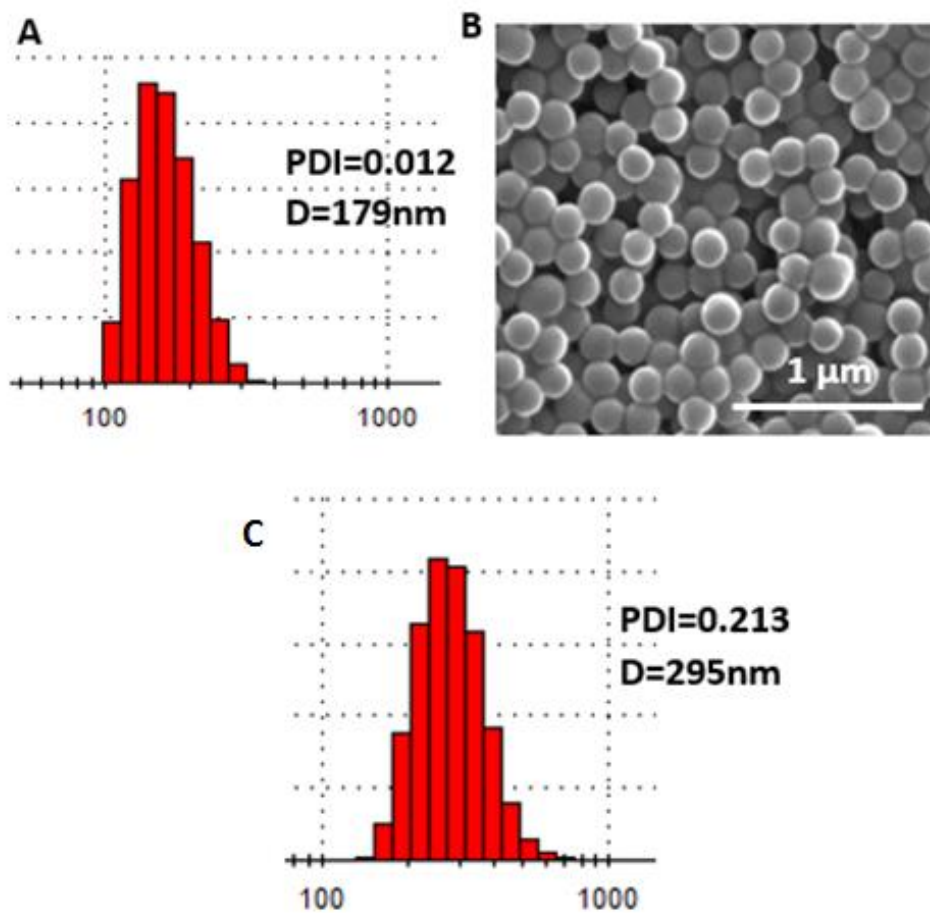


Figure 2: DLS (A) and SEM data (B) for the silica nanoparticles and DLS data for hydrazine-SNs (C).

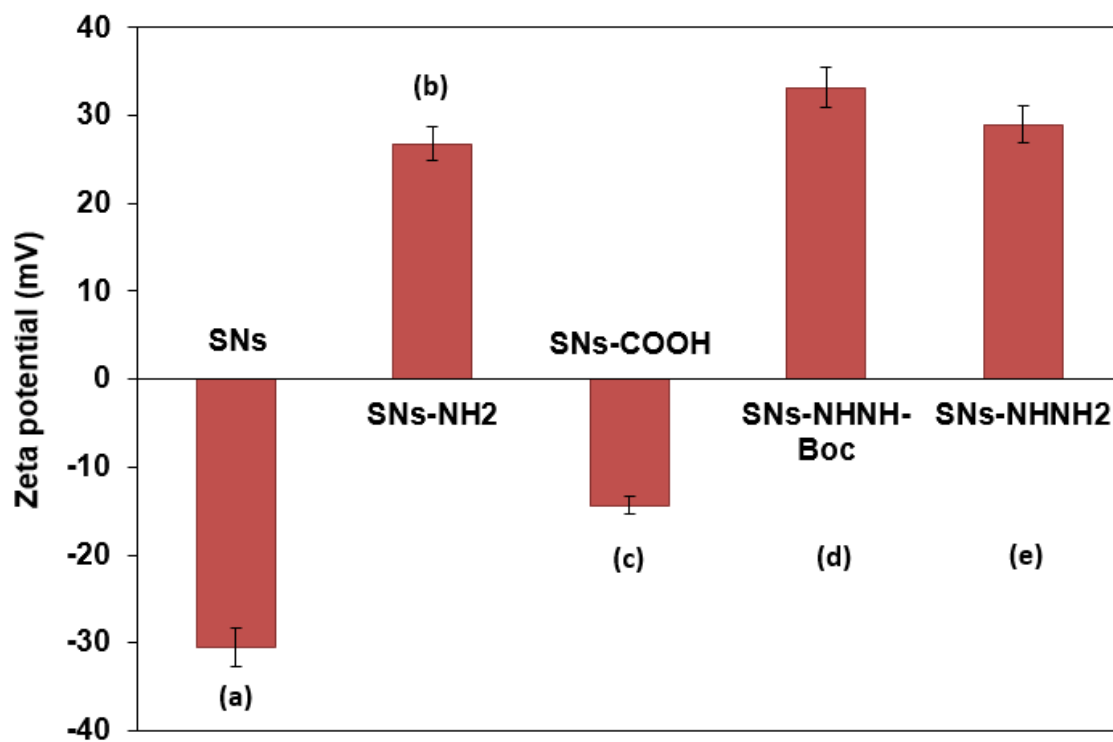


Figure 3: Zeta potentials of (a) silica nanoparticles, (b) amine functionalized SNs, (c) carboxyl functionalized SNs, (d) Boc-hydrazine-SNs and (e) hydrazine-SNs.

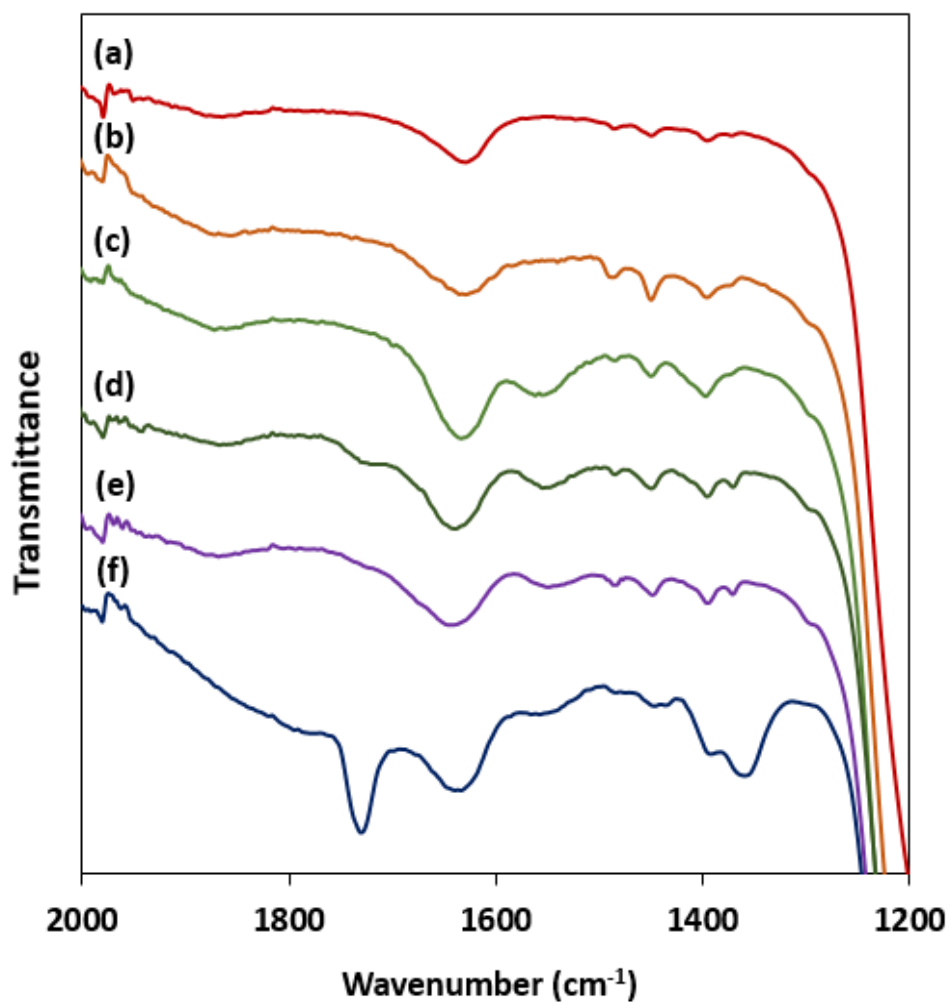


Figure 4: FTIR spectra of (a) silica nanoparticles, (b) amine functionalized SNs, (c) carboxyl functionalized SNs, (d) Boc-Hydrazine-SNs, (e) hydrazine-SNs and (f) DOX-hydrazone-SNs.

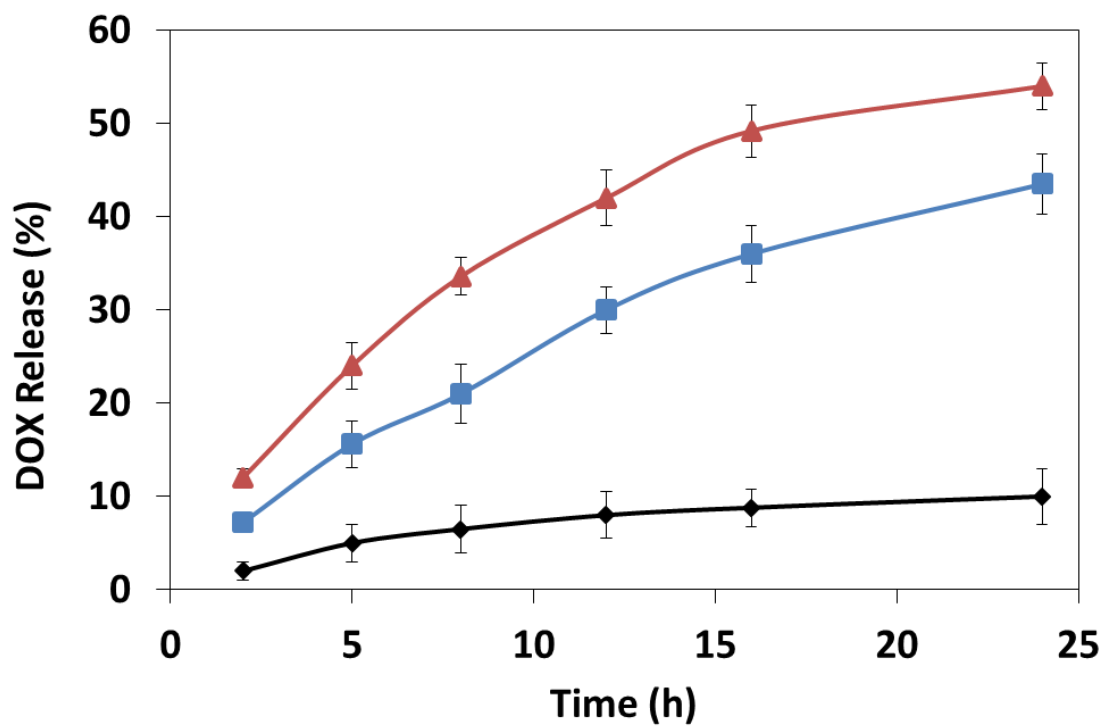


Figure 5: Drug release percentage from DOX-hydrazone-SNs at (◆) pH 7.4, (■) pH 6.5 and (▲) pH 5.0.

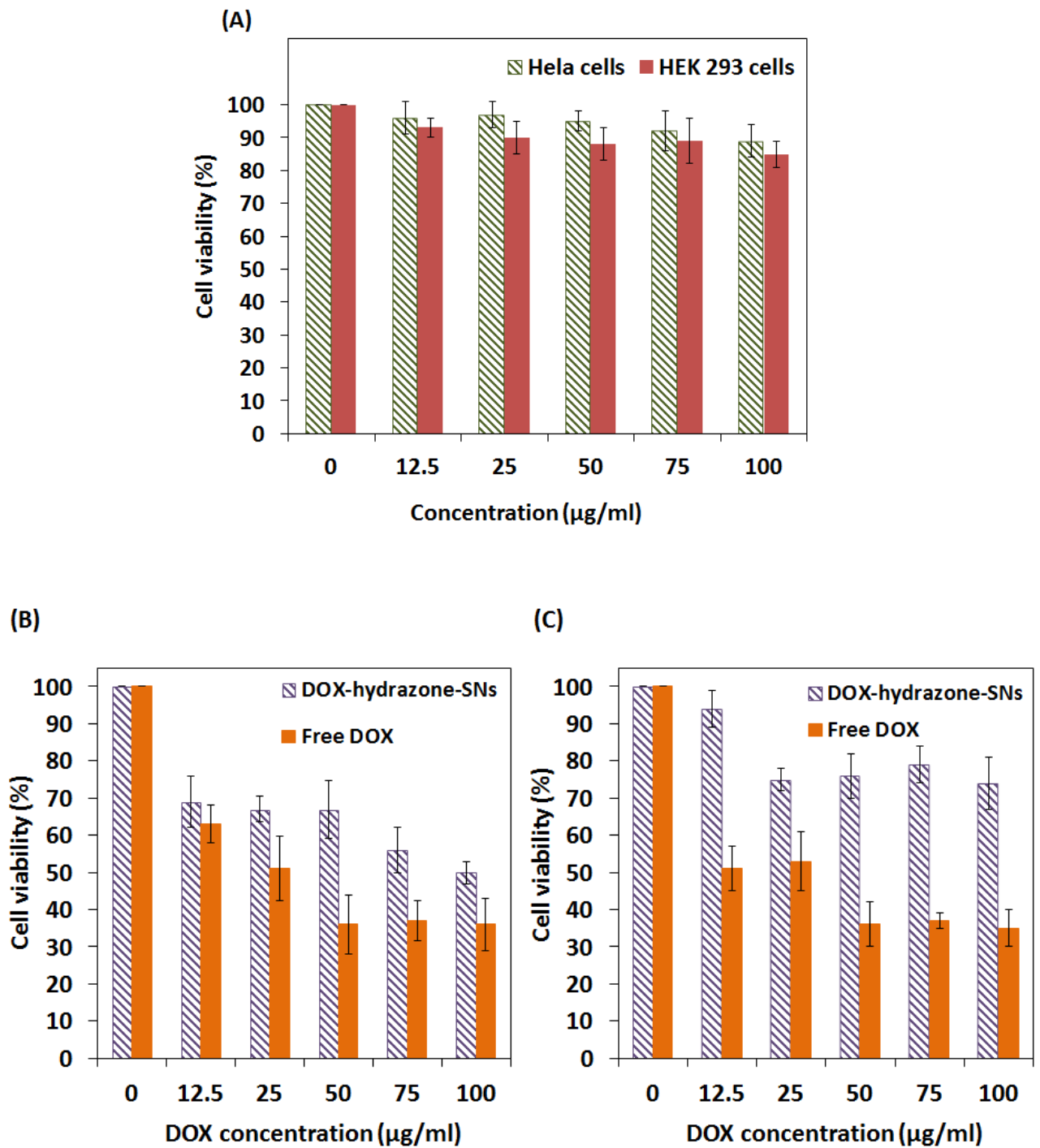


Figure 6: (A) Cytotoxicity of hydrazine-SNs against HeLa cells and HEK 293 cells, and comparative cytotoxic studies of DOX-hydrazine-SNs and free DOX against (B) HeLa cells and (C) HEK 293 cells.

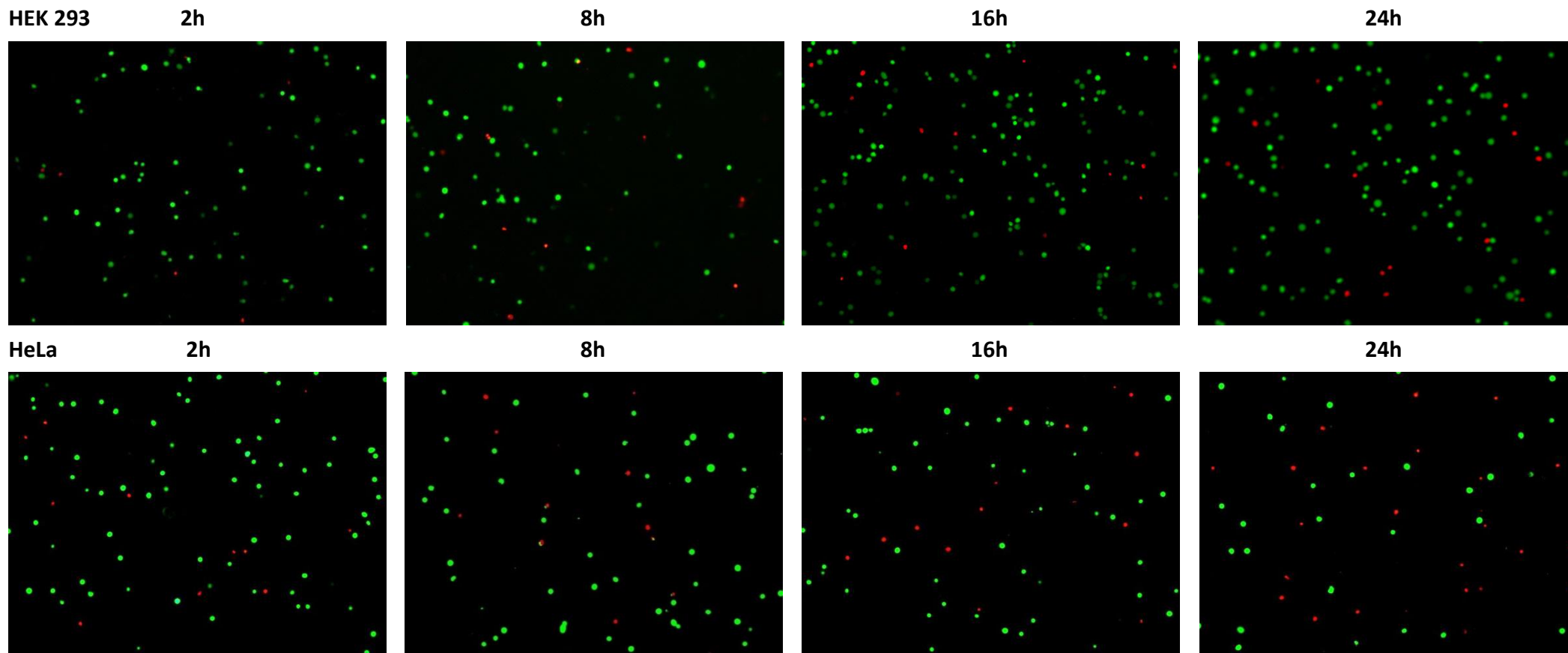
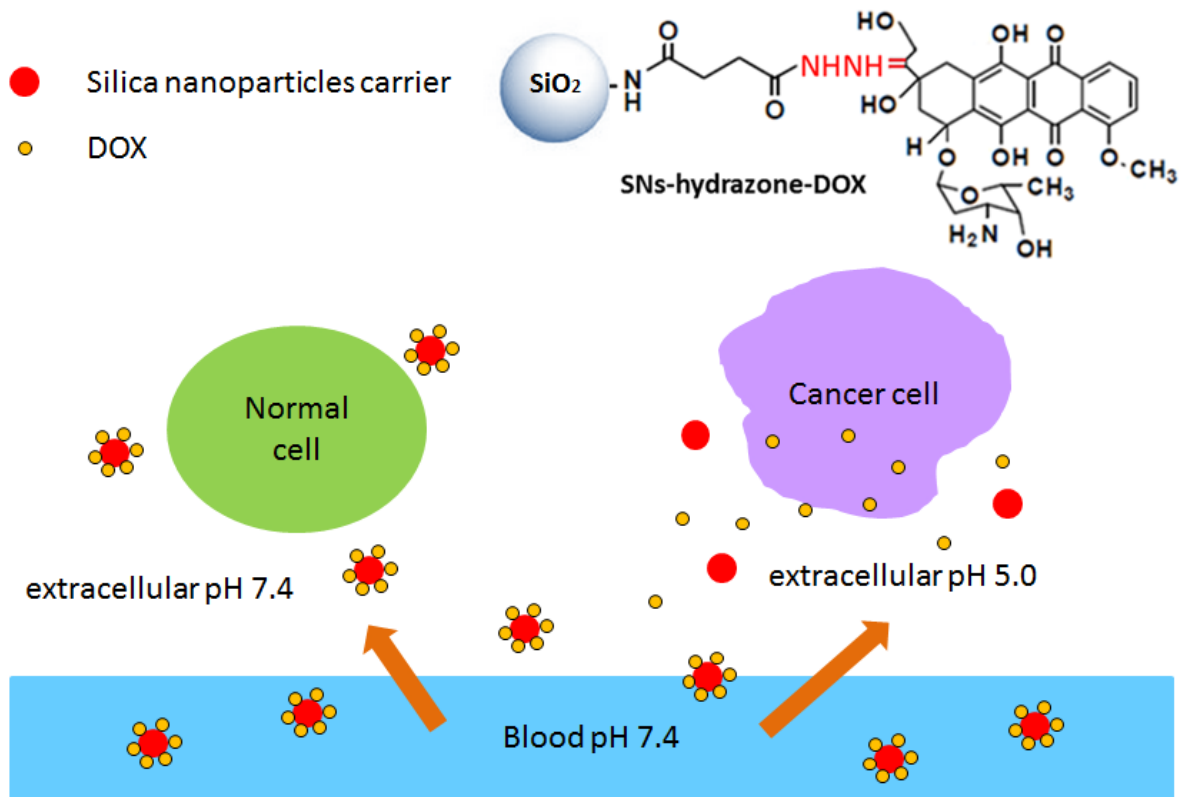


Figure 7: Fluorescence images of HEK 293 cells and HeLa cells after 2 h, 8 h, 16 h and 24 h incubation with DOX-hydrazone-SNs. The concentration of DOX-hydrazone-SNs used is 100 $\mu\text{g}/\text{ml}$. The red fluorescence represents dead cells, and the green fluorescence represents live cells.

Table of Contents Graphic



References

1. J. H. Park, G. Saravanakumar, K. Kim and I. C. Kwon, *Advanced Drug Delivery Reviews*, 2010, **62**, 28-41.
2. I. Slowing, J. L. Vivero-Escoto, C. W. Wu and V. S. Lin, *Advanced Drug Delivery Reviews*, 2008, **60**, 1278-1288.
3. C. Lu, B. Li, N. Liu, G. Wu, H. Gao and J. Ma, *RSC Advances*, 2014, **4**, 50301-50311.
4. P. DeMuth, M. Hurley, C. Wu, S. Galanie, M. R. Zachariah and P. DeShong, *Microporous and Mesoporous Materials*, 2011, **141**, 128-134.
5. A. Popat, J. Liu, G. Q. Lu and S. Z. Qiao, *Journal of Materials Chemistry*, 2012, **22**, 11173-11178.
6. Y. Cui, H. Dong, X. Cai, D. Wang and Y. Li, *ACS Applied Materials & Interfaces*, 2012, **4**, 3177-3183.
7. C. Loira-Pastoriza, J. Todoroff and R. Vanbever, *Advanced Drug Delivery Reviews*, 2014, **75**, 81-91.
8. D. W. Dong, S. W. Tong and X. R. Qi, *Journal of Biomedical Materials Research. Part A*, 2013, **101**, 1336-1344.
9. C. Du, D. Deng, L. Shan, S. Wan, J. Cao, J. Tian, S. Achilefu and Y. Gu, *Biomaterials*, 2013, **34**, 3087-3097.

10. G. M. Dubowchik, R. A. Firestone, L. Padilla, D. Willner, S. J. Hofstead, K. Mosure, J. O. Knipe, S. J. Lasch and P. A. Trail, *Bioconjugate Chemistry*, 2002, **13**, 855-869.
11. Y. Shi, H. Zhang, Z. Yue, Z. Zhang, K. S. Teng, M. J. Li, C. Yi and M. Yang, *Nanotechnology*, 2013, **24**, 375501-375508.
12. L. M. Kaminskas, B. D. Kelly, V. M. McLeod, G. Sberna, D. J. Owen, B. J. Boyd and C. J. Porter, *Journal of Controlled Release*, 2011, **152**, 241-248.
13. Y. Malam, M. Loizidou and A. M. Seifalian, *Trends in Pharmacological Sciences*, 2009, **30**, 592-599.
14. M. Colilla, B. González and M. Vallet-Regí *Biomaterials Science*, 2013, **1**, 114-134.
15. T. L. Andresen, D. H. Thompson and T. Kaasgaard, *Molecular Membrane Biology*, 2010, **27**, 353-363.
16. P. J. H. Chen, H. Shang, C. S. Hsiao, Y. Y. Chen, D. M. Liu and S. Y. Chen, *Journal of Materials Chemistry*, 2011, **21**, 2535-2543.
17. K. Kono, S. Nakashima, D. Kokuryo, I. Aoki, H. Shimomoto, S. Aoshima, K. Maruyama, E. Yuba, C. Kojima, A. Harada and Y. Ishizaka, *Biomaterials*, 2011, **32**, 1387-1395.
18. J. Z. Du, X. J. Du, C. Q. Mao and J. Wang, *Journal of the American Chemical Society*, 2011, **133**, 17560-17563.

19. A. Thistlethwaite, D. Leeper, D. Moylan III and R. Nerlinger, *Radiation Oncology Biology Physics*, 1985, **11**, 1647-1652.
20. N. G. Yabbarov, G. A. Posypanova, E. A. Vorontsov, S. I. Obydenny and E. S. Severin, *Journal of Controlled Release*, 2013, **168**, 135-141.
21. N. Lavignac, J. L. Nicholls, P. Ferruti and R. Duncan, *Macromolecular Bioscience*, 2009, **9**, 480-487.
22. C. Wang, P. Lv, W. Wei, S. Tao, T. Hu, J. Yang and C. Meng, *Nanotechnology*, 2011, **22**, 415101-415108.
23. M. Prabakaran, J. J. Grailer, S. Pilla, D. A. Steeber and S. Gong, *Biomaterials*, 2009, **30**, 5757-5766.
24. D. C. Wu, C. R. Cammarata, H. J. Park, B. T. Rhodes and C. M. Ofner, *Pharmaceutical Research*, 2013, **30**, 2087-2096.
25. X. Hu, R. Wang, J. Yue, S. Liu, Z. Xie and X. Jing, *Journal of Materials Chemistry*, 2012, **22**, 13303-13310.
26. K. P. Koutroumanis, R. G. Holdich and S. Georgiadou, *International Journal of Pharmaceutics*, 2013, **455**, 5-13.
27. J. Fan, G. Fang, X. Wang, F. Zeng, Y. Xiang and S. Wu, *Nanotechnology*, 2011, **22**, 455102-455112.

28. Y. Yu, C. K. Chen, W. C. Law, E. Weinheimer, S. Sengupta, P. N. Prasad and C. Cheng, *Biomacromolecules*, 2014, **15**, 524-532.
29. S. Aryal, J. J. Grailer, S. Pilla, D. A. Steeber and S. Gong, *Journal of Materials Chemistry*, 2009, **19**, 7879-7884.
30. K. O. Yu, C. M. Grabinski, A. M. Schrand, R. C. Murdock, W. Wang, B. Gu, J. J. Schlager and S. M. Hussain, *Journal of Nanoparticle Research*, 2008, **11**, 15-24.
31. X. Mei, D. Chen, N. Li, Q. Xu, J. Ge, H. Li and J. Lu, *Microporous and Mesoporous Materials*, 2012, **152**, 16-24.

Supporting information

Doxorubicin conjugated silica nanoparticles: A pH regulated delivery system for controlled and sustained drug release

Wanxia Zhao, Xiaolin Cui, Hu Zhang, Jingxiu Bi*, and Sheng Dai*

School of Chemical Engineering, The University of Adelaide, Adelaide SA 5005 Australia

* To whom corresponding should be addressed

email s.dai@adelaide.edu.au and jingxiu.bi@adelaide.edu.au.

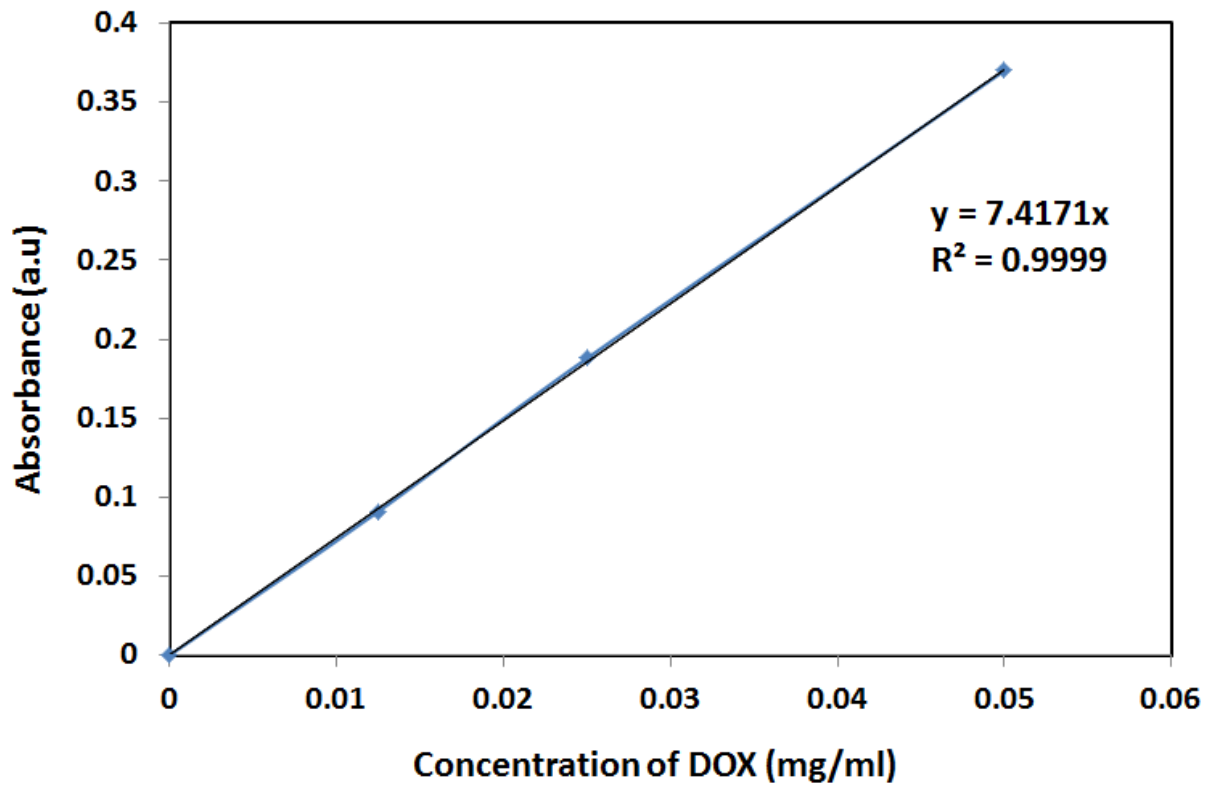


Figure S1: Calibration curve of DOX in phosphate buffer solution.

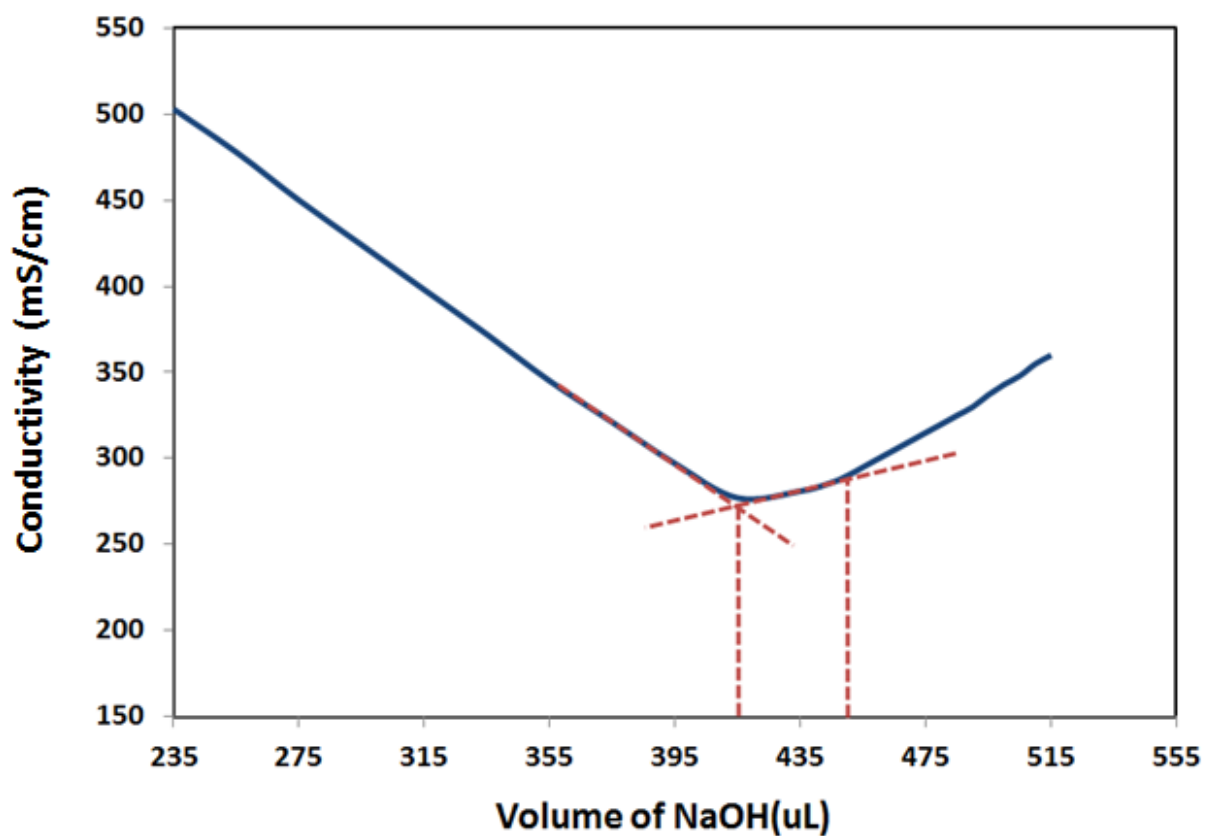


Figure S2: Conductometric titration of the amino groups on the surface of silica nanoparticles. The measurement result is 0.648mmol/g.

**Chapter 4 Intracellular microenvironment redox-responsive
drug-conjugated silica nanoparticles for sustainable drug
delivery**

Intracellular microenvironment redox-responsive drug-conjugated silica nanoparticles for sustainable drug delivery

Wanxia Zhao, Xiaolin Cui, Hu Zhang, Jingxiu Bi* and Sheng Dai*

School of Chemical Engineering, The University of Adelaide, Adelaide SA 5005 Australia

* To whom corresponding should be addressed

email s.dai@adelaide.edu.au and jingxiu.bi@adelaide.edu.au.

Statement of Authorship

Title of Paper	Intracellular microenvironment redox-responsive drug-conjugated silica nanoparticles for sustainable drug delivery
Publication Status	<input type="checkbox"/> Published <input type="checkbox"/> Accepted for Publication <input type="checkbox"/> Submitted for Publication <input checked="" type="checkbox"/> Publication Style
Publication Details	Will submit to RSC Advances.

Principal Author

Name of Principal Author (Candidate)	Wanxia Zhao		
Contribution to the Paper	Preformed experiments, analysed results, interpreted data and wrote manuscript.		
Overall percentage (%)	85%		
Signature		Date	

Co-Author Contributions

By signing the Statement of Authorship, each author certifies that:

- iv. the candidate's stated contribution to the publication is accurate (as detailed above);
- v. permission is granted for the candidate to include the publication in the thesis; and
- vi. the sum of all co-author contributions is equal to 100% less the candidate's stated contribution.

Name of Co-Author	Xiaolin Cui		
Contribution to the Paper	Assisted in experiments.		
Signature		Date	

Name of Co-Author	Hu Zhang		
Contribution to the Paper	Assisted in writing manuscript.		
Signature		Date	

Name of Co-Author	Jingxiu Bi		
Contribution to the Paper	Supervised development of work.		
Signature		Date	

Name of Co-Author	Sheng Dai		
Contribution to the Paper	Supervised development of work and assisted in writing manuscript.		
Signature		Date	

Abstract

Due to high cytotoxicity and low solubility of most anticancer drugs, various delivery systems have to be used to improve therapeutic efficiency. For conventional drug delivery systems, the drug loading by physical adsorption always results in to drug leakage and burst release. In order to overcome this problem, covalently conjugating drugs to their delivery carriers via microenvironment-responsive smart linkers has been taken into consideration. Herein, we reported a redox-responsive drug-carrier conjugation system for controlled drug delivery, where silica nanoparticles were chosen as a model carrier and doxorubicin (DOX) was selected as a model drug. The intracellular-responsive system was established by introducing dithiodibutyric acid (DTDB) to silica nanoparticle surfaces, where the disulphide bonds were responsive to glutathione (GSH). Through the cleavage of smart linkers, the conjugated anticancer drugs of DOX on the surface of silica nanoparticles can be released. Our results revealed the redox-responsive drug-carrier conjugation system was strongly responsive to the presence of reducing reagents such as glutathione (GSH) and dithiothreitol (DTT). After reduction of the disulphide bonds, the preloaded DOX could be released sustainably. On the other hand, in the absence of reduction reagent, the drug-carrier conjugation system showed good stability to prevent the undesired drug leakage during blood circulation. Our study clearly demonstrated that SNs-S-S-DOX conjugates with selectively redox responsiveness were ideal in the applications of future controlled drug delivery.

4.1 Introduction

Doxorubicin (DOX) is a widely used anticancer drug to inhibit the growth and spread of cancer cells.^{1, 2} Nevertheless, its therapeutic efficiency improvement is always obstructed by the low solubility and specificity, which contributes to numerous adverse side effects.³ Various strategies on how to delivery DOX have been developed, where controlled drug delivery system has presented impressive results to enhance therapeutic efficiency and minimize side effects of anticancer drugs.⁴⁻⁶ For an ideal controlled drug delivery system, the preloaded drugs can be delivered to target cells without premature drug release. To date, various delivery systems ranging from inorganic to organic materials have been reported.^{5, 7-9} Among them, silica nanoparticles have been considered as the feasible carriers due to their high biocompatibility and multifunctional surfaces.^{10, 11} Conventional strategies to construct silica nanoparticle based delivery systems are to load drug molecules via physical interactions, such as diffusion, electrostatic interaction, hydrophobic interaction etc.^{3, 5, 12} Singh et al. coated the surfaces of mesoporous silica nanoparticles using cross-linked poly(ethylene glycol) (PEG) shells to control the release of physically loaded DOX in the response of proteases.¹³ Due to the weak and instable physical interactions, this approach always bears the obvious disadvantage of uncontrolled burst release.^{14, 15} When triggered by stimuli, most of the drug molecules are released within a short period. Therefore, the conjugation of drug molecules and delivery carriers using an intercellular-responsive smart linker has attracted lots of attention since it can effectively provide advantages of sustainable drug release and avoid drug

leakage.^{16, 17}

Intracellular microenvironment responsive drug delivery system is to use intracellular molecules as the stimuli to trigger drug release because of their biological activities and outstanding biorecognition. In such a drug delivery system, the loaded drugs will be able to be cleaved by changing intercellular conditions and release the drugs to cytoplasm.^{3, 4} Among intracellular stimuli, the reducing agent has been widely used to construct various redox responsive delivery systems due to its higher concentration in cancer cells. Most of the redox responsive delivery systems were developed based on the introduction of disulfide bonds, which can be reduced in the presence of reducing agent, such as dithiothreitol (DTT) or glutathione (GSH).¹⁸ Since the concentration of GSH in the cytoplasm of tumours is around 8-20 mmol/l, which is 100-1000 higher than that in the blood, and 2-10 higher than that in normal cells.^{19, 20} The huge difference of GSH concentration makes the disulphide bonds be stable in blood circulation and easily cleaved in cancer cells.^{21, 22} To date, many redox responsive delivery systems have been developed based on polymeric materials and dendrimers.²³⁻²⁵ However, the applications on inorganic materials including silica nanoparticles are rarely reported.

In this study, we developed a redox responsive drug-carrier conjugation system using monodisperse silica nanoparticles as a typical carrier and DOX as the model drug. The surface of silica nanoparticles was first functionalized with disulphide linkers and then conjugated DOX covalently. In the absence of GSH or DTT, limited drug release can be observed, while at high concentrations of GSH or DTT, the cleavage of disulphide bonds

gives rise to significant drug release. *In vitro* investigation has been adopted to examine carrier cytotoxicity and cell uptake, and it is expected that this redox responsive system is a feasible candidate in the application of controlled and sustained release.

4.2 Materials and Methods

4.2.1 Materials

Doxorubicin hydrochloride (DOX) was purchased from Beijing Huafeng United Technology Co.,Ltd. Tetraethyl orthosilicate (TEOS), 3-aminopropyltriethoxysilane (APTES), toluene, dithiodibutyric acid (DTDB), sulfo-N-hydroxysuccinimide (sulfo-NHS), 1-ethyl-3-(3-dimethylaminopropyl) carbodiimide hydrochloride (EDC), DL-dithiothreitol solution (DTT) and glutathione (GSH) were purchased from Sigma-Aldrich. Ammonia aqueous (30 %) was from VWR International Pty Ltd. Ethanol and dimethyl sulphoxide (DMSO) were from Chem-Supply. Phosphate buffered saline (PBS) solution (pH 7.4, 10 \times), Dulbecco's modified Eagle medium (DMEM), fetal bovine serum (FBS), penicillin streptomycin (PS), 3-(4,5-Dimethylthiazol-2-yl)-2,5-diphenyltetrazolium bromide (MTT) reagent, LIVE/DEAD[®] viability/cytotoxicity kit (containing calcein-AM and ethidium homodimer-1), cell culture flasks and well plates were all purchased from Life Technologies Australia Pty Ltd. Water was obtained from a Milli-Q water purification system with the resistivity of more than 18.2 M Ω ·cm.

4.2.2 Synthesis of monodisperse silica nanoparticles

A modified Stöber method was applied to prepare monodisperse silica nanoparticles (SNs).²⁶ In a typical experiment, 2.5 ml ammonia aqueous and 1.5 ml Milli-Q water were added into 50 ml anhydrous ethanol. The mixture was placed in a water bath and maintained at 40 °C for 20 min. After that, 1.5 ml TEOS was quickly charged into the mixture and reacted for another 12 h. The obtained white-colour precipitates were centrifuged and washed with ethanol and water for three times to remove any reaction residual. The washed silica nanoparticles were dispersed in anhydrous ethanol for storage.

4.2.3 Synthesis of redox sensitive linker modified silica nanoparticles

The above synthesized silica nanoparticles were first modified by introducing surface amino groups. 100 mg purified silica nanoparticles were dispersed in 40 ml anhydrous toluene. Under the protection of nitrogen, 0.15 ml APTES was added into the mixture quickly and then refluxed at 110 °C for 16 h. After cooling down to room temperature, the precipitates were washed 3 times by ethanol to obtain the amino group functionalized silica nanoparticles (SNs-NH₂).

The redox responsive linkers were conjugated to the surface of silica nanoparticles through the formation of amide bonds.²⁷ In details, 11 mg dithiodibutyric acid (DTDB) was dissolved in 10 ml PBS solution (5× concentrate) followed by adding 18 mg NHS and 18 mg EDC to active its carboxyl groups for 30 min. The mixture of 20 mg SNs-NH₂

and 5 ml PBS solution was dropwise added into the carboxyl-activated DTDB solution, and continued to stir for 24 h. The obtained disulphide linker modified silica nanoparticles (SNs-S-S-COOH) were washed by ethanol and water, and finally redispersed in anhydrous ethanol for future use.

4.2.4 Drug conjugation and *ex vivo* drug release evaluation

The conjugation of DOX to the redox responsive linker modified silica nanoparticles were carried out through EDC coupling.^{28, 29} 12 mg purified SNs-S-S-COOH particles were dissolved in 10 ml PBS solution. 22 mg EDC and 22 mg NHS were added to the solution to activate the surface carboxyl groups on silica nanoparticles. After 30 min, 5 ml PBS solution containing 1.5 mg DOX hydrochloride was slowly charged, and the mixture was allowed to stir for another 24 h at room temperature in darkness. The final product was washed 3 times with ethanol to remove unreacted DOX to get the red colored DOX conjugated silica nanoparticles (SNs-S-S-DOX).

The amount of unreacted DOX in the mixture was examined by a UV-visible spectrophotometer at the wavelength of 480 nm and compared with a standard calibration curve of DOX in PBS solution (Figure S1). The drug loading efficiency on silica nanoparticles could be calculated using the equation:

$$\begin{aligned} & \text{Drug loading efficiency (\%)} \\ & = \frac{\text{DOX weight in feed-unreacted DOX weight in the solution}}{\text{weight of DOX conjugated silica nanoparticles}} \times 100\% \quad (1) \end{aligned}$$

To evaluate the *ex vitro* drug release behaviours upon responsiveness to redox system, 5 mM and 10 mM GSH and DTT in PBS buffer solution were prepared. 5 mg of SNs-S-S-DOX conjugates were dispersed in 10 ml PBS buffer solutions with different concentrations of GSH and DTT, and the mixtures were stirred in darkness. In order to examine the release kinetics of DOX, 1 ml of aliquot was taken from the aqueous phase at the time intervals of 2 h, 4 h, 6 h and 8 h, and then replaced with 1 ml GSH/DTT PBS solution to keep volume constant. The absorbance of the aliquot samples was monitored by a UV-visible spectrophotometer at the wavelength of 480 nm, and the released DOX was able to be quantified via the calibration curve of DOX in PBS. All experiments were repeated for three times, and the values of mean \pm SD were reported.

4.2.5 Cytotoxicity

The cytotoxicity of the redox responsive linker modified silica nanoparticles and the DOX conjugated silica nanoparticles were performed by MTT assays. The cell lines used to examine cytotoxicity included human cervical cancer HeLa cells and human embryonic kidney HEK 293 cells. The cells were seeded into a 96-well plate at a density of 5.0×10^4 cells/well and incubated with 150 μ l DMEM growth medium containing 1 % PS and 10 % FBS at 37 °C. The samples of surface modified silica nanoparticles, DOX conjugated silica nanoparticles and free DOX were prepared at different concentrations, where the equivalent DOX concentrations were from 0 to 1.25 μ g/ml. After incubating cells in the 96-well plate for 24 h, the growth medium was replaced with the fresh one

containing 11 μl above samples, and the samples of each concentration were repeated for 4 times. Following 24 h further incubation, 10 μl MTT was added to each well. After another 4 h culturing, the growth medium was replaced by 150 μl DMSO in order to dissolve the formed formazan crystals. The absorbance was then measured by a microplate reader at the wavelength of 595 nm, and the cell viability was presented as the percentage based on active viable cells.

4.2.6 Fluorescent Dead/Live cell assays

HeLa cells or HEK 293 cells were seeded into a 24-well plate with the density of 2.5×10^5 cells per well at 24 h before the experiment. 10 μg drug conjugated silica nanoparticles was added into each well after replacing the growth medium by 150 μl fresh one. With further incubation of 2 h, 6 h and 10 h, the fluorescence microscope was used to monitor cell viability. The cell samples were washed by PBS solution for three times, followed by being stained with 400 μl fluorescence staining reagent, which contained 2 μM calcein-AM and 4 μM ethidium homodimer-1, for 30 min. After washing, the cells were observed using a fluorescence microscope, where the calcein in live cells produced green fluorescence at 488 nm and the ethidium homodimer-1 in dead cells produced red fluorescence at 530 nm.

4.2.7 Equipment

Dynamic light scattering (DLS) and zeta potential were measured by a Malvern Zetasizer Nano ZS (ZEN 3600). Fourier transform infrared (FTIR) spectra were taken by a Thermo Scientific Nicolet 6700 FTIR spectrometer at room temperature. UV-vis absorption spectra were obtained by a Shimadzu UV-Visible spectrophotometer (UV-1601), and the standard calibration curve of DOX in PBS solution was established at 480 nm (Figure S1). Evaluation of cell viability by MTT assays was measured using an ELx808 Absorbance Microplate Reader from BioTek. Florescent emission and excitation images were recorded on a ZEISS Axion Vert.A1 inverted fluorescence microscope. The live cells were viewed using green fluorescent port filter with excitation wavelength of 470 ± 20 nm and emission wavelength of 525 ± 25 nm, while the dead cells were viewed using DsRed filter with excitation wavelength of 545 ± 13 nm and emission wavelength of 605 ± 35 nm.

4.3 Results and Discussion

4.3.1 Preparation and characterization of SNs-S-S-DOX conjugates

The SNs-S-S-DOX conjugates were prepared through the procedure detailed in Figure 1, which involved silica surface amino modification, redox-responsive linker functionalization and DOX conjugation. Silica nanoparticles (SNs), the biocompatible drug delivery carriers, were synthesised by a modified Stöber method. The abundant

silanol groups, Si–OH, on nanoparticle surface render the SNs well disperse in aqueous system. SNs were further modified to introduce surface amino functional groups in order to conjugate redox sensitive linkers. The purified silica nanoparticles were reacted with 3-aminopropyltriethoxysilane (APTES) to obtain the amino group modified silica nanoparticles (SNs-NH₂). The modification is through the reaction between the amino groups of APTES and the Si–OH groups under anhydrous or polar alcoholic condition.³⁰

The redox sensitive linker, DTDB, contains one redox responsive disulphide group and two carboxylic acid groups. It was introduced to the surface of amino-modified silica nanoparticles by EDC coupling in a 5 × PBS (pH = 7.4) solution. DTDB shows good solubility and stability in the PBS solution, and the treatment of EDC and NHS allows its activated carboxyl groups react with the amino groups on silica nanoparticle surface through the formation of amide bonds. Due to the presence of two carboxyl groups of DTDB, largely excess amount of DTDB (molar ratio of DTDB to amino groups on silica nanoparticles = 10:1) was used to ensure only one carboxyl group on the DTDB be reacted with amino groups to prevent multiple particles aggregation,²⁷ while the other unreacted carboxyl group of DTDB is ready to be used as the functional groups for further DOX conjugation. In the final step, the NHS activated carboxyl groups on DTDB modified silica nanoparticles react with the amino groups of DOX to achieve covalently drug loading. Under the presence of reductant, the disulphide bonds might be cleaved to release the preloaded drugs.

The hydrodynamic sizes of various silica nanoparticles were measured by dynamic light

scattering (DLS) as shown in Table 1. The hydrodynamic diameter of silica nanoparticles (SNs) before surface modification is 163 nm, while the diameter after amino group and redox sensitive linker modification are 276 nm and 283 nm. The significant size increase after surface modifications is associated with different hydration of these functional groups, i.e. carboxyl groups and amino groups have stronger hydration effect than hydroxyl groups.

Fourier transform infrared spectroscopy (FTIR) spectra were recorded to obtain information on silica nanoparticle surface modification. As shown in Figure 2, the peak at 1490 cm^{-1} in the spectrum of SNs-NH₂ is attributed to the bending of the primary amine groups modified on silica nanoparticles surfaces. After coupling the redox sensitive linker, the formation of new peptide bonds between the amino groups on silica nanoparticle surfaces and the carboxyl groups on the DTDB linker gives rise to the new peak at 1530 cm^{-1} , while the absorption peak of amide groups become weaken. The vibration peak of the disulphide bonds overlaps with the strong silanol peak at 900 cm^{-1} . The above characterization results indicate that the redox sensitive linker modified silica nanoparticles have been synthesised successfully.

Zeta potentials of these surface modified silica nanoparticles were measured to further confirm these functional groups have been introduced to the surface of SNs. As shown in Table 1, the zeta potential of SNs in water before chemical modification is -49.0 mV , which is due to the ionization of Si-OH groups. After amino group modification, the zeta potentials change to $+26.1\text{ mV}$ due to the protonation of amino groups. After introducing

the redox responsive linkers, the presence of surface carboxyl groups leads zeta potential change to -16.8 mV. These zeta potential values indicate the stability of these SNs in aqueous system.

The carboxyl groups on the surface of redox sensitive linkers modified silica nanoparticles provide reactive sites for further drug conjugation. DOX was conjugated to silica nanoparticles by EDC chemistry. In order to improve conversion, the redox sensitive linker modified silica nanoparticles (SNs-S-S-COOH) were treated with NHS for carboxyl group activation. The formed semi-stable NHS amides make it more reactive with the amino groups of DOX. After DOX conjugation, the colour of silica nanoparticles changes from white to red. From Table 1, the zeta potential of the SN-S-S-DOX conjugates becomes + 20.3 mV due to the presence of positively charged DOX molecules. The particle size of 178 nm clearly indicates no aggregation is formed after conjugation. These results demonstrate that DOX has been covalently conjugated to the surface of silica nanoparticles through a redox-responsive smart linker.

4.3.2 *Ex vivo* redox-responsive triggered cleavage of the SNs-S-S-DOX conjugates by DTT and GSH

In order to examine the redox-responsive drug release of the SNs-S-S-DOX conjugates, dithiothreitol solution (DTT) and glutathione (GSH) are chosen as typical reducing stimuli to trigger the release of DOX. Both DTT and GSH are biological reducing agents widely used to reduce disulphide bonds in biological applications. In the presence of DTT

or GSH, the disulphide linkage of the DOX conjugated silica nanoparticles can be reduced. After cleavage of the disulphide bonds, the preloaded DOX drugs will be released to the medium gradually. The *ex vivo* drug release behaviour was evaluated based on the absorbance changing of DOX in the PBS solution containing different concentrations of DTT/GSH, being measured by a UV-visible spectrophotometer at 480 nm.

From Figure 3, it is clear that in the control group without DTT and GSH, the DOX conjugated silica nanoparticles show good stability in PBS where less than 10 % of drugs release. In contrast, adding 10 mM DTT or GSH, the conjugated DOX can be released effectively from silica nanoparticle surfaces during the first 8 h, and the highest accumulated drug release are 51 % and 47 %. In addition, comparing the release profiles of 5mM and 10mM DTT or GSH, the amount of drugs released is proportional to the concentrations of these reducing agents in solution. High concentration of reducing agent accelerates drug release. The above observation suggests that DTT and GSH can effectively reduce the disulphide bonds to release the preloaded drugs being conjugated on the surfaces of silica nanoparticles. On the other hand, the results also indicate the sustained drug release profiles of the DOX conjugated silica nanoparticles, where DOX is released gradually and continually within 8 h. Since the concentration of GSH in cancer cell cytoplasm is 100 to 1000 higher than that in blood plasm. The disulphide linked drug-carriers conjugates will be stable during blood circulation and cleaved inside cancer cells to achieve the smart intracellular microenvironment triggered drug release. Since

the drug release is triggered by the cleavage of disulphide linkages, it prolongs the duration of drug release than the drugs being physically adsorbed. With the help of sustained release, the drug concentration in cancer cells can maintain at an effective level over a long time so as to improve the efficiency in cancer therapy.

4.3.3 *In vitro* evaluation of cytotoxicity and cell uptake against HeLa cells and HEK 293 cells

In order to evaluate the effectiveness of this drug delivery system *in vitro*, the cytotoxicities of SNs-S-S-DOX conjugates against cancer cells (HeLa cells) and normal cells (HEK 293 cells) were investigated. The cell viabilities after the treatment with SNs-S-S-COOH, DOX conjugated silica nanoparticles (SNs-S-S-DOX) and free DOX were determined through MTT assays, where the pale yellow MTT can only be converted to the blue formazan crystals by the mitochondrial enzymes in viable cells. From Figure 4, SNs-S-S-COOH does not show cytotoxicity to both HeLa cells and HEK 293 cells with the viability more than 90 %, which indicates the inorganic drug carriers are biocompatible and safe for drug delivery applications. From Figure 5, the presence of DOX conjugated silica nanoparticles leads to significant cell growth inhibition for both cells, but the cell inhibition of HEK 293 cells is less than that of HeLa cells due to their different GSH concentrations. When incubating both cells with 100 µg/ml SNs-S-S-DOX conjugates (equivalent to 1.25 µg/ml of doxorubicin), the viability of HeLa cells decreases to 65 %, but the viability of HEK 293 cells drops to 75 %. Since the GSH

concentration in the cytoplasm of tumours is 2-10 higher than that in normal cells, the cell viability difference demonstrates that our drug delivery systems are associated with different GSH levels of various cells. The released DOX is dependent on the concentration of intracellular GSH. When treated cells with SNs-S-S-DOX conjugates, the GSH in cells microenvironment cleaves the disulphide bond and release the conjugated DOX to inhibit cell growth, whereas the low concentration of GSH in the blood makes the disulphide linker difficult to break and thus safe during the course of delivery. Moreover, compared with the cell viability after being incubated with free DOX, the drug loaded silica nanoparticles presents less cytotoxicity to both cells. For HEK 293 cells, the cell viability of DOX conjugated silica nanoparticles is 75 %, while the cell viability of free DOX is 57 %. It is suggest that by using SNs-S-S-DOX conjugates as a drug delivery system, the cytotoxicity of anticancer drugs to normal cells can be reduced and make it more feasible in the applications of cancer treatments.

On the other hand, in order to further evaluate the redox sensitive drug release of the SNs-S-S-DOX conjugates, the live/dead cell assays were used to analyse cell uptake behaviours. Both HeLa cells and HEK 293 cells were incubated with 100 µg/ml SNs-S-S-DOX conjugates in DMEM growth medium, and the florescence images were taken at the incubation time points of 2 h, 6 h and 10 h respectively. The cells were further stained by calcein-AM and ethidium homodimer-1 dyes, where the green florescence intensity indicates live cells and the red florescence intensity indicates dead cells. From Figure 6, we can find that after the incubation of 2 h, few red florescence can be observed

in both HeLa cells and HEK 293 cells. It means the most of cells are still alive. With long time incubation, the red fluorescence of HeLa cells and HEK 293 cells display considerable increase, which indicates the toxicity of cleaved DOX from silica nanoparticles surface. After 10 h incubation, approximate 25 % of red fluorescence can be observed in HeLa cells, higher than that for HEK 293 cells of 10 %. This result indicates the released DOX is associated with the concentration of intracellular GSH. Since the cytoplasm of cancer cells contain higher level of GSH than normal cells, more DOX can be released in cancer cells, which resulting the lower cell viability. The live/dead cell assays agree with the MTT results. The increase of red fluorescence intensity of HeLa cells is gradually between each time period. It implies DOX experiences the sustainable drug release within 10 h, which is in agreement with the result of *ex vivo* drug release study in PBS solution. Therefore, the results further prove the possibility of controlled and sustained drug release using the smart SNs-S-S-DOX systems.

4.4 Conclusions

In this study, the redox responsive DOX conjugated silica nanoparticles have been synthesised using disulphide bonds as the smart linker. After the surface functionalization of silica nanoparticles with DTDB, DOX were conjugated to the low cytotoxic carriers (SNs-S-S-COOH) by EDC coupling. The *ex vivo* drug release study shows that the disulphide bonds are stable in the absence of DTT or GSH, while with the existence of DTT or GSH, the disulphide bonds can be reduced to release preloaded drug sustainably.

From the *in vitro* MTT and live/dead cell assays, our drug delivery system can release DOX in different cells and more DOX can be released in cancer cells due to their higher intracellular GSH concentrations. Therefore, our results suggest this smart delivery system provides the possibility for future applications of sustainable drug release without leakage during the delivery course.

Acknowledgments

This work was financially supported by the Australian Research Council (ARC) Discovery Projects (DP140104062 and DP110102877).

Supporting Information Available

The calibration curve of DOX is available in supporting information.

Table 1: Characterization of various silica nanoparticles with and without surface modification.

Samples	Particle size (nm)	PDI	Zeta potential (STD) (mV)
SNs	163	0.026	-49.0 (0.52)
SNs-NH ₂	276	0.091	+26.1 (0.72)
SNs-S-S-COOH	283	0.183	-16.8 (0.47)
SNs-S-S-DOX	178	0.096	+20.3 (0.56)

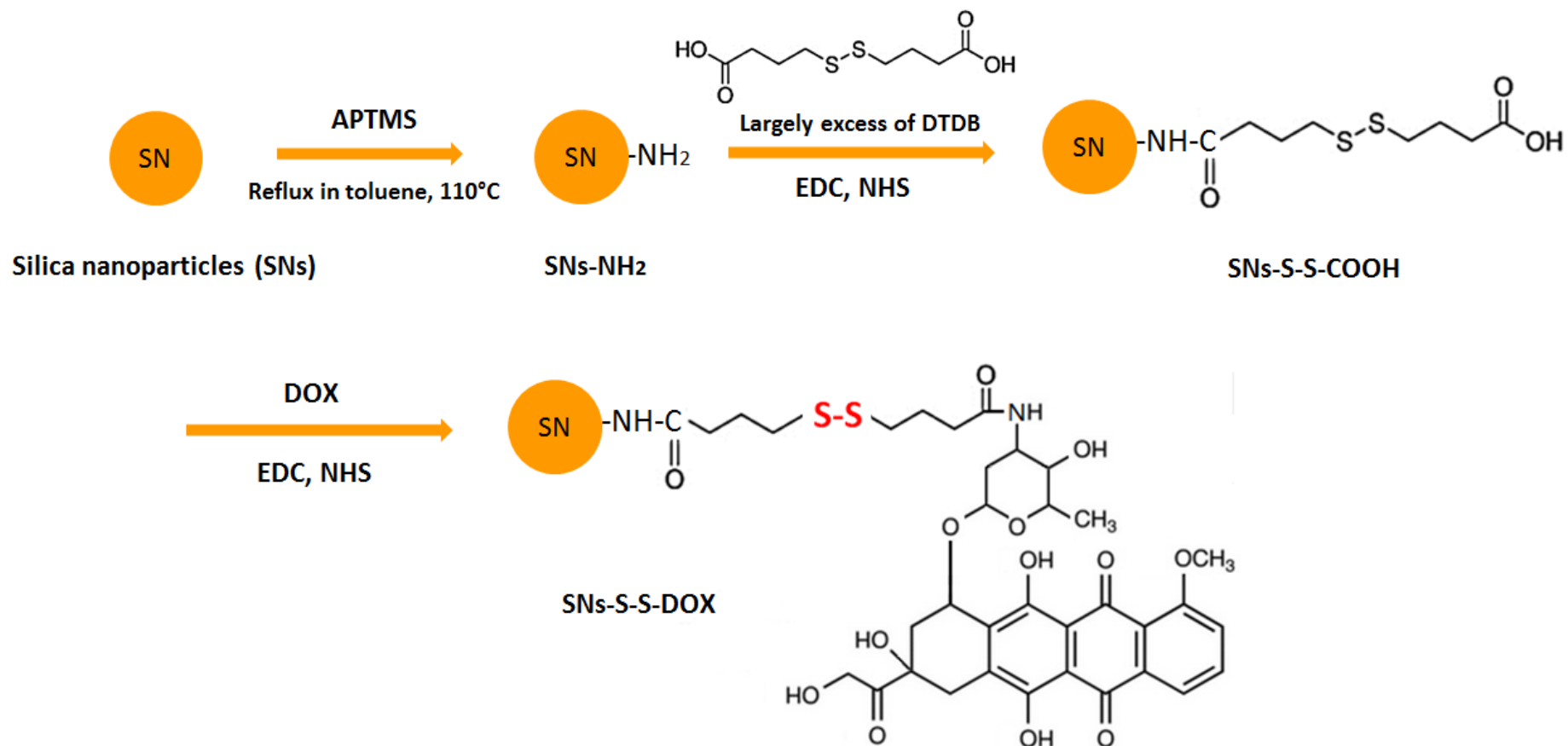


Figure 1: Synthesis scheme of DOX conjugated silica nanoparticles with a redox sensitive linker.

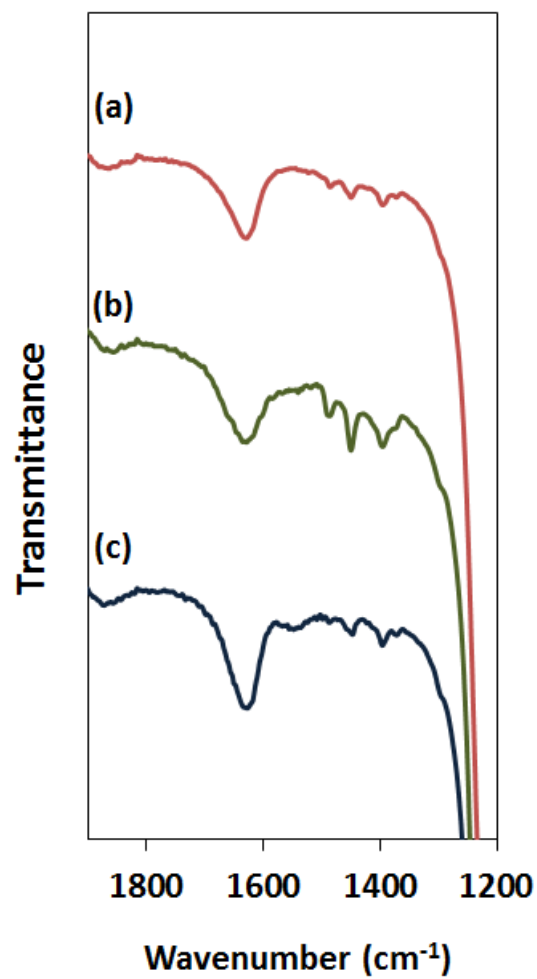


Figure 2: FTIR spectra of (a) silica nanoparticles (SNs), (b) amine functionalized SNs (SNs-NH₂), (c) redox sensitive linker modified silica nanoparticles (SNs-S-S-COOH).

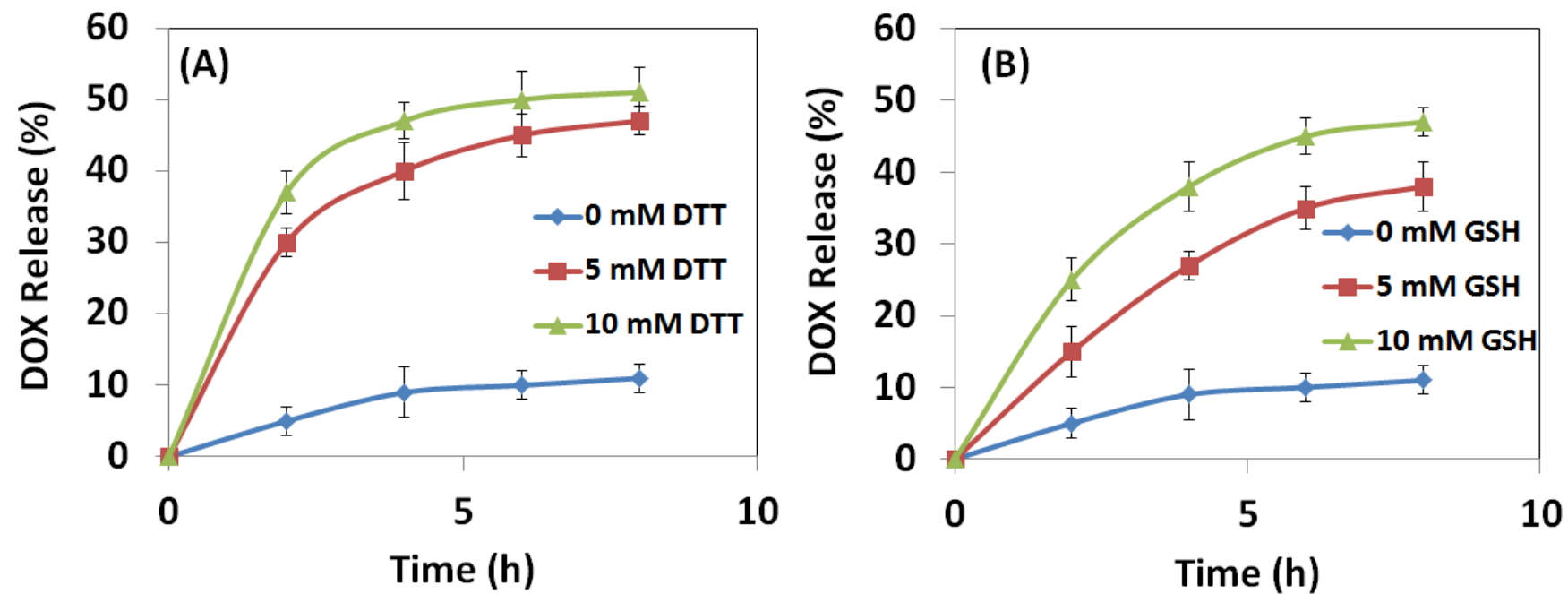


Figure 3: Time dependent DOX release behaviors of SNs-S-S-DOX in the PBS solutions (pH 7.4) with different concentrations of (A) DTT and (B) GSH.

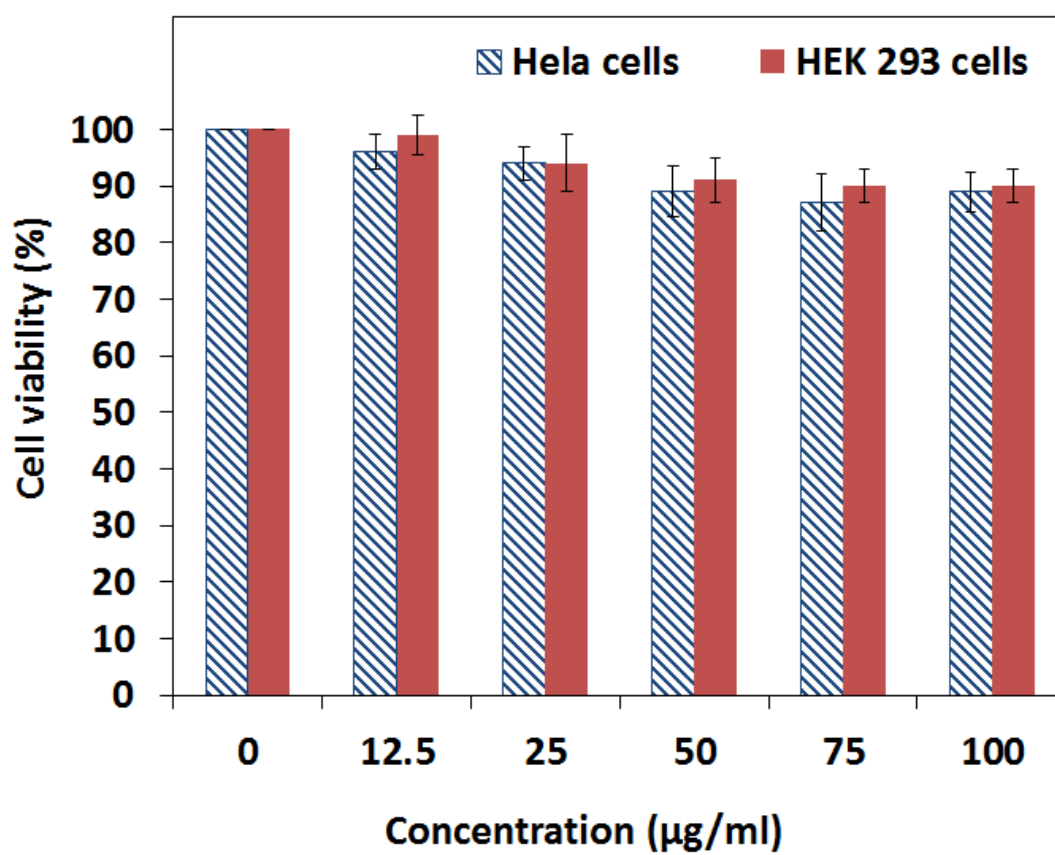


Figure 4: Cytotoxicity of SNs-S-S-COOH carrier against HeLa cells and HEK 293 cells.

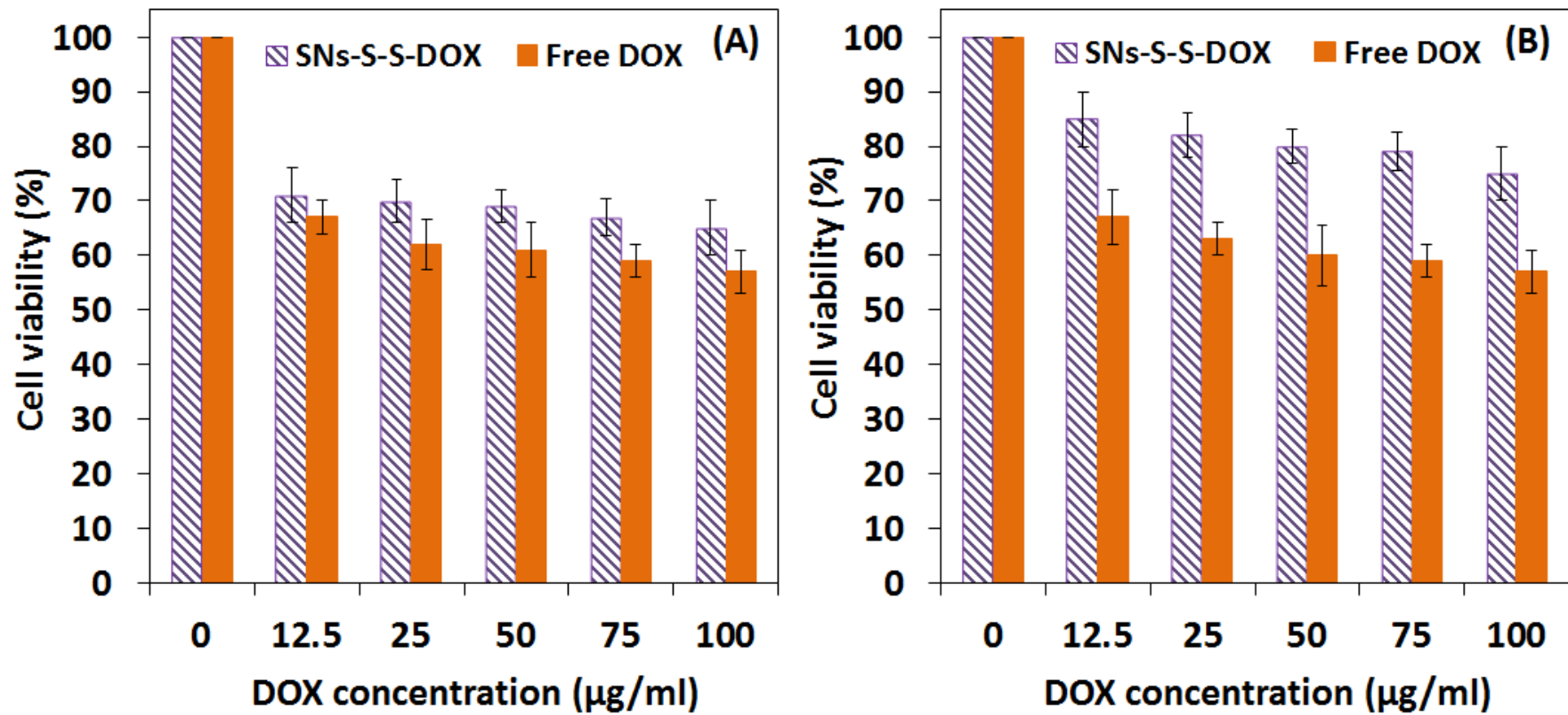
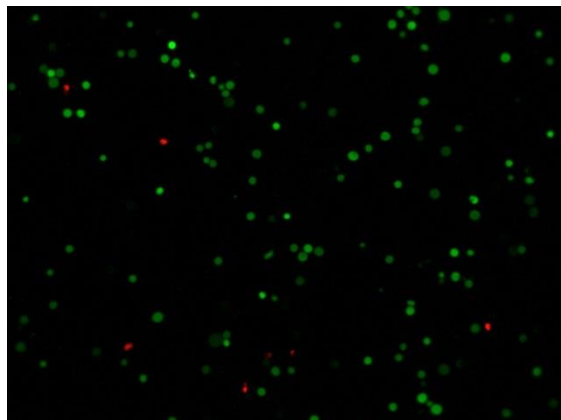


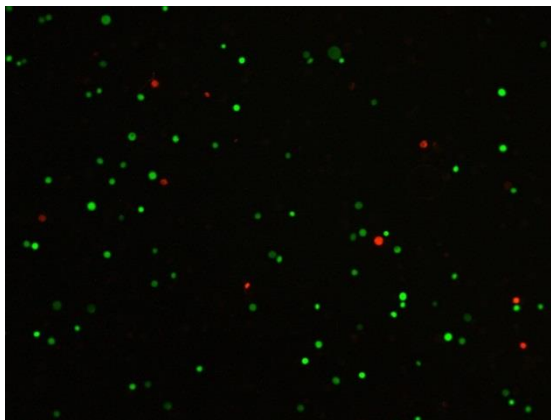
Figure 5: Cell viability of (A) HeLa cells and (B) HEK 293 cells after being incubated with SNs-S-S-DOX conjugates and free DOX.

HEK 293 cells

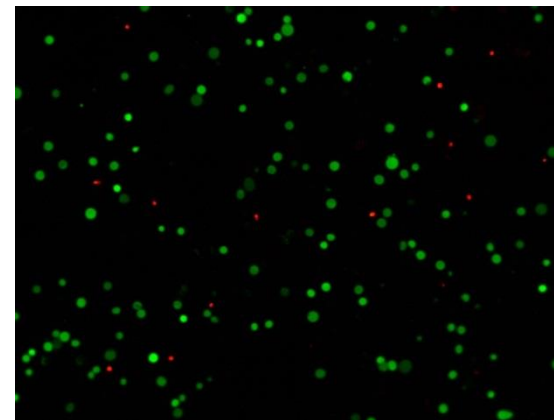
2h



6h

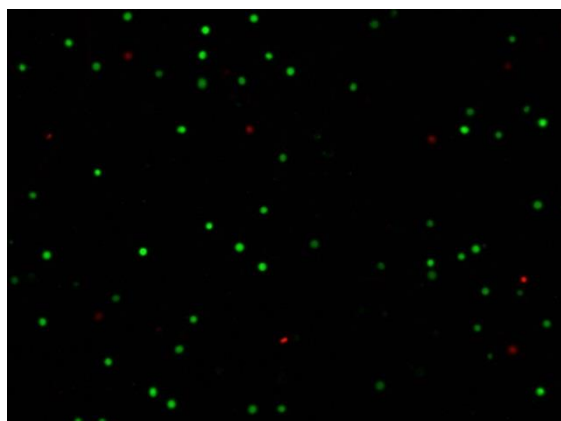


10h

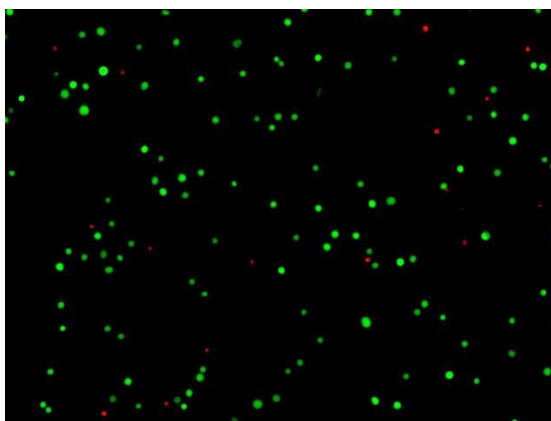


HeLa cells

2h



6h



10h

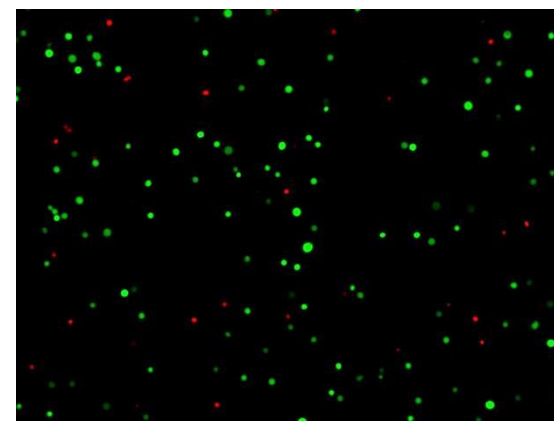
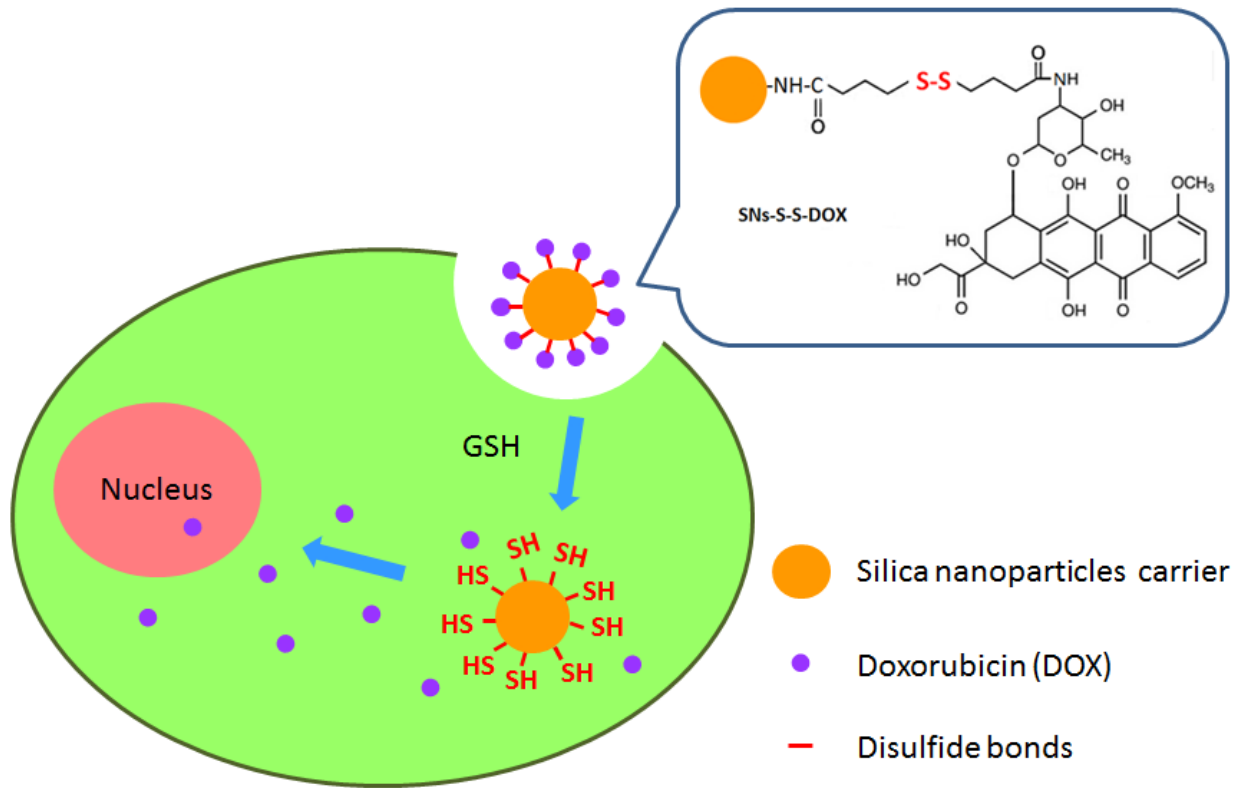


Figure 6: Fluorescence images of HEK 293 cells and HeLa cells after 2 h, 6 h and 10 h incubated with SNs-S-S-DOX.

Table of Contents Graphic



References

1. N. Z. Knezevic, B. G. Trewyn and V. S. Lin, *Chemistry*, 2011, **17**, 3338-3342.
2. C. Du, D. Deng, L. Shan, S. Wan, J. Cao, J. Tian, S. Achilefu and Y. Gu, *Biomaterials*, 2013, **34**, 3087-3097.
3. R. de la Rica, D. Aili and M. M. Stevens, *Advanced Drug Delivery Reviews*, 2012, **64**, 967-978.
4. T. L. Andresen, D. H. Thompson and T. Kaasgaard, *Molecular Membrane Biology*, 2010, **27**, 353-363.
5. M. Colilla, B. González and M. Vallet-Regí *Biomaterials Science*, 2013, **1**, 114-134.
6. F. M. Kievit, F. Y. Wang, C. Fang, H. Mok, K. Wang, J. R. Silber, R. G. Ellenbogen and M. Zhang, *Journal of Control Release*, 2011, **152**, 76-83.
7. G. M. Dubowchik, R. A. Firestone, L. Padilla, D. Willner, S. J. Hofstead, K. Mosure, J. O. Knipe, S. J. Lasch and P. A. Trail, *Bioconjugate Chemistry*, 2002, **13**, 855-869.
8. F. M. Veronese, O. Schiavon, G. Pasut, R. Mendichi, L. Andersson, A. Tsirk, J. Ford, G. Wu, S. Kneller, J. Davies and R. Duncan, *Bioconjugate Chemistry*, 2005, **16**, 775-784.
9. C. Burns, W. U. Spindel, S. Puckett and G. E. Pacey, *Talanta*, 2006, **69**, 873-876.
10. Y. Yang, J. Aw, K. Chen, F. Liu, P. Padmanabhan, Y. Hou, Z. Cheng and B. Xing, *Chemistry, an Asian Journal*, 2011, **6**, 1381-1389.

11. Y. C. Chen, X. C. Huang, Y. L. Luo, Y. C. Chang, Y. Z. Hsieh and H. Y. Hsu, *Science and Technology of Advanced Materials*, 2013, **14**, 44407-44429.
12. P. L. Lu, Y. C. Chen, T. W. Ou, H. H. Chen, H. C. Tsai, C. J. Wen, C. L. Lo, S. P. Wey, K. J. Lin, T. C. Yen and G. H. Hsiue, *Biomaterials*, 2011, **32**, 2213-2221.
13. N. Singh, A. Karambelkar, L. Gu, K. Lin, J. S. Miller, C. S. Chen, M. J. Sailor and S. N. Bhatia, *Journal of the American Chemical Society*, 2011, **133**, 19582-19585.
14. C. H. Tsai, J. L. Vivero-Escoto, Slowing, II, I. J. Fang, B. G. Trewyn and V. S. Lin, *Biomaterials*, 2011, **32**, 6234-6244.
15. P. DeMuth, M. Hurley, C. Wu, S. Galanie, M. R. Zachariah and P. DeShong, *Microporous and Mesoporous Materials*, 2011, **141**, 128-134.
16. N. Q. Shi, W. Gao, B. Xiang and X. R. Qi, *International Journal of Nanomedicine*, 2012, **7**, 1613-1621.
17. S. H. Medina, M. V. Chevliakov, G. Tiruchinapally, Y. Y. Durmaz, S. P. Kuruvilla and M. E. Elsayed, *Biomaterials*, 2013, **34**, 4655-4666.
18. X. Wu, Y. Li, C. Lin, X. Y. Hu and L. Wang, *Chemical Communications*, 2015, **51**, 6832-6835.
19. Q. Q. Tang, L. Yuan, D. Yang and J. H. Hu, *Acta Chimica Sinica*, 2010, **68**, 1925-1929.
20. H. Li, J. Z. Zhang, Q. Tang, M. Du, J. Hu and D. Yang, *Materials Science & Engineering. C, Materials for Biological Applications*, 2013, **33**, 3426-3431.

21. Y. Chang, K. Yang, P. Wei, S. Huang, Y. Pei, W. Zhao and Z. Pei, *Angew Chem Int Ed Engl*, 2014, **53**, 13126-13130.
22. H. Gong, Z. Xie, M. Liu, H. Zhu and H. Sun, *RSC Advances*, 2015, **5**, 59576-59582.
23. A. Zhang, Z. Zhang, F. Shi, C. Xiao, J. Ding, X. Zhuang, C. He, L. Chen and X. Chen, *Macromol Bioscience*, 2013, **13**, 1249-1258.
24. S. Ghosh, V. Yesilyurt, E. N. Savariar, K. Irvin and S. Thayumanavan, *Journal of Polymer Science. Part A, Polymer Chemistry*, 2009, **47**, 1052-1060.
25. T. B. Ren, W. J. Xia, H. Q. Dong and Y. Y. Li, *Polymer*, 2011, **52**, 3580-3586.
26. I. Slowing, J. L. Vivero-Escoto, C. W. Wu and V. S. Lin, *Advanced Drug Delivery Reviews*, 2008, **60**, 1278-1288.
27. X. Du, B. Shi, Y. Tang, S. Dai and S. Z. Qiao, *Biomaterials*, 2014, **35**, 5580-5590.
28. Y. Shi, H. Zhang, Z. Yue, Z. Zhang, K. S. Teng, M. J. Li, C. Yi and M. Yang, *Nanotechnology*, 2013, **24**, 375501-375508.
29. Q. Zhao, W. Chen, Y. Chen, L. Zhang, J. Zhang and Z. Zhang, *Bioconjugate Chemistry*, 2011, **22**, 346-352.
30. H. S. Jung, D. S. Moon and J. K. Lee, *Journal of Nanomaterials*, 2012, **2012**, 1-8.

Supporting information

Intracellular microenvironment redox-responsive drug-conjugated silica nanoparticles for sustainable drug delivery

Wanxia Zhao, Xiaolin Cui, Hu Zhang, Jingxiu Bi* and Sheng Dai*

School of Chemical Engineering, the University of Adelaide, Adelaide SA 5005 Australia

* To whom corresponding should be addressed

email s.dai@adelaide.edu.au and jingxiu.bi@adelaide.edu.au.

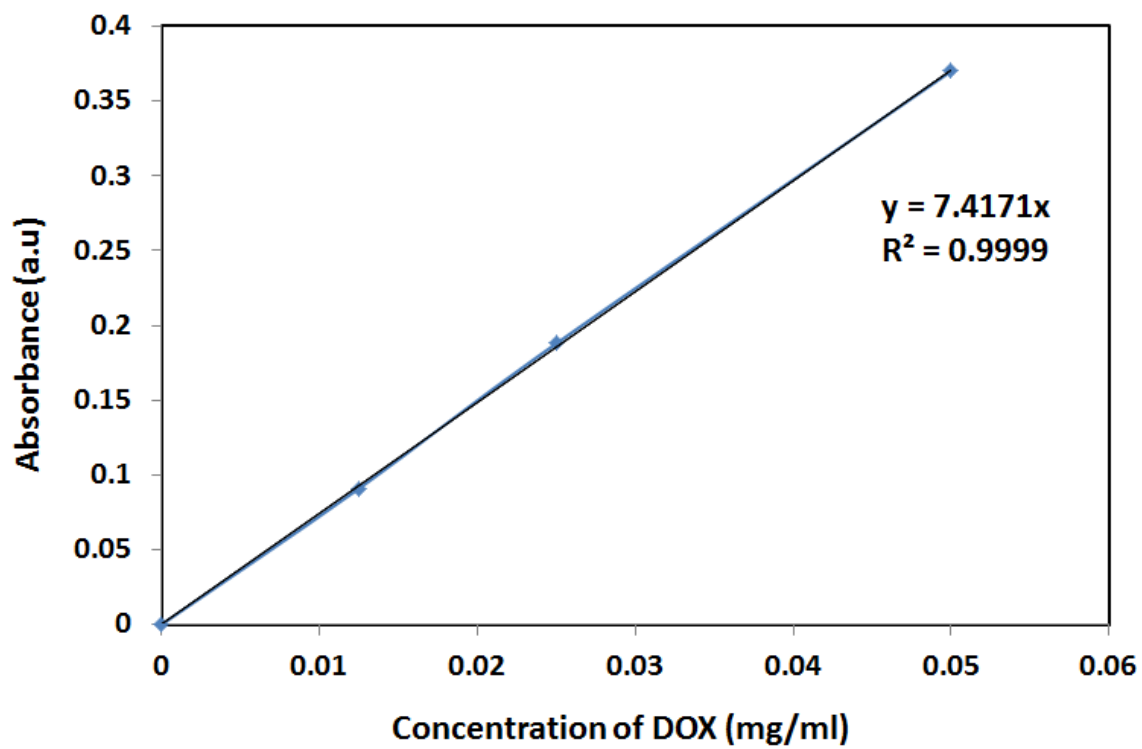


Figure S1: Calibration curve of DOX in phosphate buffer solution.

Chapter 5 Conclusions and Recommendation

5.1 Conclusions

This work focuses on the syntheses and evaluation of the pH responsive drug delivery systems with hydrazone bonds and the intracellular microenvironment redox responsive drug delivery systems with disulfide bonds. Silica nanoparticles are chosen as the model carriers, and a variety of surface modification has been carried out so as to covalently conjugate a model anticancer drug of doxorubicin.

Modified st öber approach was used to synthesize uniform silica nanoparticles within the size of 160 - 180 nm. For the pH sensitive drug delivery systems, the linkers of tert-butyl carbazate were introduced to the surface of silica nanoparticles by EDC coupling, and then reacted with the ketonic group of DOX to form the pH-responsive hydrazone bonds. The functionalized carriers before drug loading are not cytotoxic. After drug loading, the pH responsive drug conjugate systems show good stability under the physiological pH of 7.4 and sustainable drug release under the low pH conditions associated with the hydrolysis of hydrazone bonds. Apart from inhibiting cancer cell grown, such drug delivery systems can also minimize the side effects of anticancer drugs to normal tissues.

On the other hand, for the intracellular microenvironment redox responsive drug delivery systems, the DTDB that containing disulfide bonds was chosen as the smart linker to establish redox responsive drug-carrier conjugation systems. Both the carboxyl groups of

DTDB were reacted with the amino group on silica nanoparticles and the amino groups of DOX by step EDC coupling reactions to form amide bonds. In the drug release study, the loaded DOX can be effectively released in the presence of intracellular reduction reagents, such as GSH. The higher concentration of reduction reagents, the more rapid drug release can be observed. Such intracellular micro-environment responsive drug delivery systems with redox sensitive linkers can be used to effectively prevent the premature leakage during circulation, and controlled release drugs to different cells.

When comparing the drug release and cell uptake behaviors of these two delivery systems, both of them show the outstanding ability in controlled drug release. In the neutral environment or the absence of reduction agent, both drug delivery systems are stable without premature drug leakage, which means they can be stable in blood circulation. Based on their different release profiles, the pH sensitive system seems to have better performance in sustainable release. For the redox sensitive system, almost all of the loaded drugs are released within 8 h, but for the pH sensitive system, the drugs can experience longer time up to 16 h, which will be able to prolong the time of effective concentrations. Moreover, due to the existence of certain amount of GSH in normal cells, although its concentration is 2-10 times lower than that in tumors, which makes the redox responsive drug delivery system have less targeting ability as good as the pH sensitive system.

5.2 Future recommendation

Based on current research results, for the future development, in first place, active targeting ligands can be introduced to the carriers of redox responsive drug delivery systems to improve its targeting ability, and reduce the drug cytotoxicity to normal cells. In addition, different smart linkers, such as enzyme-responsive systems, can be applied to the silica nanoparticles to compare with our current results, and different drug molecules rather than DOX, can be loaded to study their delivery and release performances. Moreover, traceable drug delivery systems can also be launched to obtain more details on the drug/carrier separation after cell endocytosis. Finally, the cytotoxicity of synthesized drug conjugated silica nanoparticles can be further assessed by *in vivo* tumor inhibition experiment. The mouse model animal test can be conducted to evaluate the *in vivo* bio-distribution of drug molecules as well as the tumor inhibition efficiency by imaging the volume change of excised organs.